

# Aharonov-Bohm Interferometry with Interacting Quantum Dots: Spin Configurations, Asymmetric Interference Patterns, Bias-Voltage-Induced Aharonov-Bohm Oscillations, and Symmetries of Transport Coefficients

Jürgen König<sup>1,2</sup> and Yuval Gefen<sup>3</sup>

<sup>1</sup>*Institut für Theoretische Festkörperphysik, Universität Karlsruhe, 76128 Karlsruhe, Germany*

<sup>2</sup>*Department of Physics, The University of Texas at Austin, Austin, Texas 78712, USA*

<sup>3</sup>*Department of Condensed Matter Physics, The Weizmann Institute of Science, 76100 Rehovot, Israel*

(October 29, 2018)

We study electron transport through multiply connected mesoscopic geometries containing interacting quantum dots. Our formulation covers both equilibrium and nonequilibrium physics. We discuss the relation of coherent transport channels through the quantum dot to flux-sensitive Aharonov-Bohm oscillations in the total conductance of the device. Contributions to transport in first and second order in the intrinsic linewidth of the dot levels are addressed in detail. We predict an interaction-induced asymmetry in the amplitude of the interference signal around resonance peaks as a consequence of incoherence associated with spin-flip processes. This asymmetry can be used to probe the total spin of the quantum dot. Such a probe requires less stringent experimental conditions than the Kondo effect, which provides the same information. We show that first-order contributions can be partially or even fully coherent. This contrasts with the sequential-tunneling picture, which describes first-order transport as a sequence of incoherent tunneling processes. We predict bias-voltage-induced Aharonov-Bohm oscillations of physical quantities which are independent of flux in the linear-response regime. Going beyond the Onsager relations we analyze the relations between the space symmetry group of the setup and the flux-dependent nonlinear conductance.

PACS numbers: 73.23.Hk, 73.63.Kv, 73.40.Gk

## I. INTRODUCTION

The manifestation of quantum coherence in finite systems is in the foundations of the physics of mesoscopic systems. The presence of quantum coherence is detectable through interference experiments, most notably Aharonov-Bohm (AB) interferometry. The prototype of an AB setup is a double-slit experiment, as shown in Fig. 1a. An electron moving from the left reservoir to the right one is split into two partial waves which interfere with each other. A magnetic flux  $\Phi$  that penetrates the area enclosed by the two paths changes the relative phase of the amplitudes of the two partial waves, which yields a flux dependence of the total transmission probability through the device.

A convenient framework to study the role of electron-electron (e-e) interactions in mesoscopic systems is suggested by employing quantum dots (QDs). The latter provide a relatively simple and controlled scheme to address e-e interactions without undermining the rich physics involved. Transport through QDs has been studied extensively and revealed interesting phenomena such as resonant tunneling, Coulomb blockade, and the Kondo effect. However, the measurement of the current through QDs does not provide information about the quantum coherence of the transport. In particular, it doesn't address the interplay of electron-electron interactions and quantum coherence. In order to approach these questions QDs have been embedded in AB geometries.<sup>1-20</sup> Magnetic-flux sensitivity of the total current has been

observed,<sup>2,7,11,12,18</sup> indicating at least partially coherent transport through the QD.

By applying a finite bias voltage across the device the QD can be driven out of equilibrium, lifting the complexity of the system to a qualitatively higher level. In the context of interacting QDs nonequilibrium effects such as splitting of Kondo resonances have been discussed. It is only natural to expect that driving the system out of equilibrium enriches the interplay between quantum coherence and interaction effects by another facet. Some of the symmetries present at equilibrium, which underline linear response, may be broken, and at the same time new qualitative features may emerge.

In this paper we address two main issues:

(i) What can we learn about QDs by embedding them into AB geometries? Based on Ref. 19, we will classify different contributions to linear transport into coherent and incoherent channels. We concentrate on the dominant transport mechanism, which is of first order in the intrinsic linewidth of the dot levels when the QD is tuned in resonance with the leads and of second order (“cotunneling”) in the Coulomb blockade regime.<sup>21</sup> A sufficient condition to establish *full* coherence is to find an AB geometry in which the interference pattern reveals *fully destructive interference* since transport processes through the QD which are *cancelled* by *adding* parallel transmission channels cannot be incoherent. As we will see the proper choice of the AB interferometer, including either one or two QDs, is important for the manifestation of this criterion.

A very important and striking result of our analysis

will lead to the suggestion that AB interferometers (with either one or two QDs) can be used to probe the total spin of the QD. We will find that the relative magnitude of the flux-dependent AB signal, the visibility, changes from one Coulomb blockade valley to the next. This amounts to an asymmetry in the AB signal around the Coulomb conductance peaks. The higher visibility indicates the side of the peak which corresponds to a situation where the QD is mostly occupied by an even number of electrons (doubly occupied levels) with a total spin 0. The lower visibility corresponds to an odd number of electrons and total spin 1/2. A similar even/odd effect in the low-temperature conductance through a QD results from the Kondo effect.<sup>22–29</sup> Thus, measurement of the conductance probes the total spin of the QD, too, although the physical origin is completely different. We stress that our spin-dependent asymmetry effect is *not* a manifestation of incipient Kondo physics. Indeed, we expect our asymmetry to disappear in the zero-temperature limit, where the Kondo effect is fully developed. In order to access the Kondo regime, low temperature and strong coupling of the dot to the leads is required. This contrasts with our suggestion to employ an AB interferometer. We predict the asymmetry of the AB signal to survive at high temperature and weak coupling, i.e., much less stringent conditions.

(ii) The other major issue of this paper addresses the interplay between quantum coherence and electron-electron interaction for systems *out of equilibrium*. In the linear-response regime the average electron number on the QD is an equilibrium quantity. For weak coupling between dot and leads (such that the intrinsic linewidth is small compared to the energy scale provided by the temperature and the level spacing), the dot occupation is governed by classical Boltzmann factors, which are independent of magnetic flux. Out of equilibrium, however, we predict *bias-voltage-induced AB oscillations* in the dot occupation for a single-dot AB interferometer. We emphasize that, again, the experimental conditions for this effect to occur, high temperature and weak coupling, are accessible rather easily.

Qualitative differences between equilibrium and nonequilibrium situations also show up in symmetry relations of transport coefficients. The classical double-slit setup (Fig. 1a) is an example of an *open-geometry* interferometer, where those electrons which are not transmitted directly to the lead on the right are absorbed by other gates and terminals of the system at the periphery of the device (these are not shown in the figure). In most parts of the paper, however, we consider AB interferometers in a *closed geometry*, as sketched in Fig. 1b, where these electrons can only go to either the terminal on the left or the one on the right-hand-side. For the open-geometry setup (Fig. 1a)  $\Phi = 0$  is *not* a symmetry point (i.e., the transmission, as well as transport coefficients and the partition function, are not invariant under  $\Phi \rightarrow -\Phi$ ). The symmetry point depends on specifics of the interferometer. This contrasts with the case of a two-terminal

geometry (Fig. 1b), where all thermodynamic potentials as well as *linear-response* transport coefficients are invariant under the inversion of the flux.<sup>30</sup> The fact that  $\Phi = 0$  is an extremum point is usually referred to as *phase locking*, and is a direct consequence of Onsager relations. It has been demonstrated<sup>5</sup> that beyond linear response, i.e., in the presence of a finite voltage bias, phase locking is, in general, broken. We show by an explicit calculation that for a two-terminal AB interferometer including a single QD *both* electron-electron interaction *and* finite bias voltage is needed to break phase locking.

But even in the nonlinear-response regime, there are symmetry relations in the transport coefficients which are connected to the space-symmetry group of the setup. This will be especially important for AB interferometers with two QDs, where, depending on the spatial symmetry, phase locking can occur even at finite bias voltages.

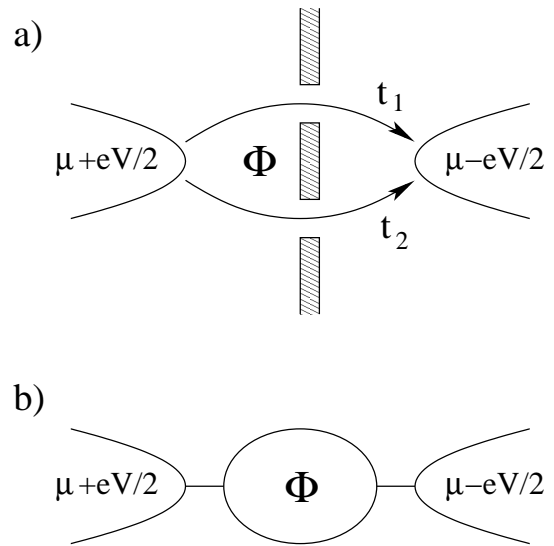


FIG. 1. a) Two-slit experiment as an open-geometry AB interferometer: only a fraction of the electrons passing through the interferometer will reach the drain. b) Two-terminal (closed-geometry) AB interferometer: all electrons injected from the source must either reach the drain or be reflected to the source.

We conclude this introduction with some remarks about the formalism to be employed. The experimentally accessible quantity which characterizes transport is the total current through the device, which is driven by bias voltage  $V$ . The electrical current (flowing from the right to the left) can be written in the form

$$I = \frac{e}{h} \sum_{\sigma} \int d\omega T_{\sigma}(\omega) [f_L(\omega) - f_R(\omega)], \quad (1.1)$$

where  $f_r(\omega) = 1/[1 + \exp(\beta(\omega - \mu_r))]$  with  $r = L/R$  is the Fermi-Dirac distribution function, and  $\beta = 1/(k_B T)$  is the inverse temperature. The left and the right lead have

fixed electrochemical potentials  $\mu_L = \mu + eV/2$  and  $\mu_R = \mu - eV/2$  for the electrons, respectively, with  $e > 0$ . The quantity  $T_\sigma(\omega)$  defines the probability for an incoming electron with energy  $\omega$  (measured with respect to  $\mu$ ) and spin  $\sigma$  to be transmitted through the device.

According to the Landauer-Büttiker or scattering formalism,<sup>31,32</sup> which we are not going to use for reasons explained below, the transmission *probability*  $T_\sigma(\omega)$  for each channel labeled by  $\omega$  and  $\sigma$  is obtained from the modulus squared of the total transmission *amplitude*. In the example of the double-slit setup, Fig. 1a, we have  $T_\sigma(\omega) = |t_{1\sigma}(\omega) + t_{2\sigma}(\omega)|^2$ , where  $t_1$  and  $t_2$  are the partial amplitudes through either slit and are complex quantities. The associated phases have an orbital contribution, determined by the geometrical details of the interferometer, and a magnetic-flux-dependent part. The transmission probability is, then, given by

$$T = |t_1|^2 + |t_2|^2 + 2|t_1 t_2| \cos(\varphi + \delta\theta), \quad (1.2)$$

where  $\delta\theta$  is the relative orbital phase,  $\varphi \equiv 2\pi\Phi/\Phi_0$  accounts for the enclosed magnet flux, and  $\Phi_0 = h/e$  is the flux quantum. (Here, for this geometry, it is justified to neglect the multiply scattered higher-winding-number amplitudes. For closed geometries, such as in Fig. 1b, the partial amplitudes may exhibit a more complicated dependence on magnetic field, representing partial amplitudes with higher winding numbers around the enclosed flux.) The success of the Landauer-Büttiker picture lies in part in the fact that, once the partial transmission amplitudes are known, the analysis is straightforward. Indeed, for *noninteracting* systems, the transmission amplitude for an electron to travel from the left to the right lead is simply determined from the (retarded) single-particle Green's function  $G_{LR,\sigma}^r(\omega)$  which involves a creation operator of an electron in the right and an annihilation operator in the left lead. *This single-particle picture, however, breaks down if electron-electron interaction is taken into account.* This has been shown in the literature<sup>33</sup> and will be explicitly demonstrated in the next section. In this case, we do not see a general recipe of how to construct meaningful transmission amplitudes.

Instead we directly calculate the current using Green's function techniques for *interacting* systems,<sup>29,33,34</sup> and extract the transmission *probability* from Eq. (1.1) without worrying about transmission amplitudes.

The outline of this paper is as follows. In Sec. II we employ a simple physical picture to distinguish coherent from incoherent transport through a QD. To substantiate these qualitative considerations we calculate in Sec. III the current through an AB interferometer in which a single QD is embedded. Interferometry with two QDs is addressed in Sec. IV. Section V is devoted to nonequilibrium physics, and in Sec. VI we draw the connection between the spatial symmetry of the setup and symmetry relations of nonlinear transport coefficients. We have also included a few appendices to provide some technical details of our analysis. In Appendix A and B we determine the density matrix for the single-dot and two-dot

AB interferometer, respectively, and in Appendix C we present an alternative derivation of Eq. (4.7).

The main results of our analysis are summarized in (i) Eqs. (3.9) and (3.12) (the zeroth and first-order expressions for the current through the interferometer); (ii) Eqs. (3.13) and (3.14) (the flux-dependent linear-response transmission for the closed and open geometry respectively); (iii) Eqs. (3.18), (3.19), (4.7), (4.8) (the absence/presence of asymmetry in the case of  $U = 0$ ,  $U = \infty$  respectively), for the single QD in the cotunneling regime, and the double QD at resonance; (iv) the various regimes for the multilevel dot indicated at the end of Section III E; (v) Eqs. (5.4) and (5.5) (the finite-bias induced AB oscillations in the dot occupation  $\langle N \rangle$ ); (vi) Eqs. (6.5) - (6.7) (the relation between flux-reversal symmetry and space-symmetry, away from linear response).

## II. COHERENT VERSUS INCOHERENT TRANSPORT THROUGH A QD

Before analyzing AB interferometers which contain QDs, as shown in Figs. 2b and c, we begin with considering transport through a QD alone, Fig. 2a.

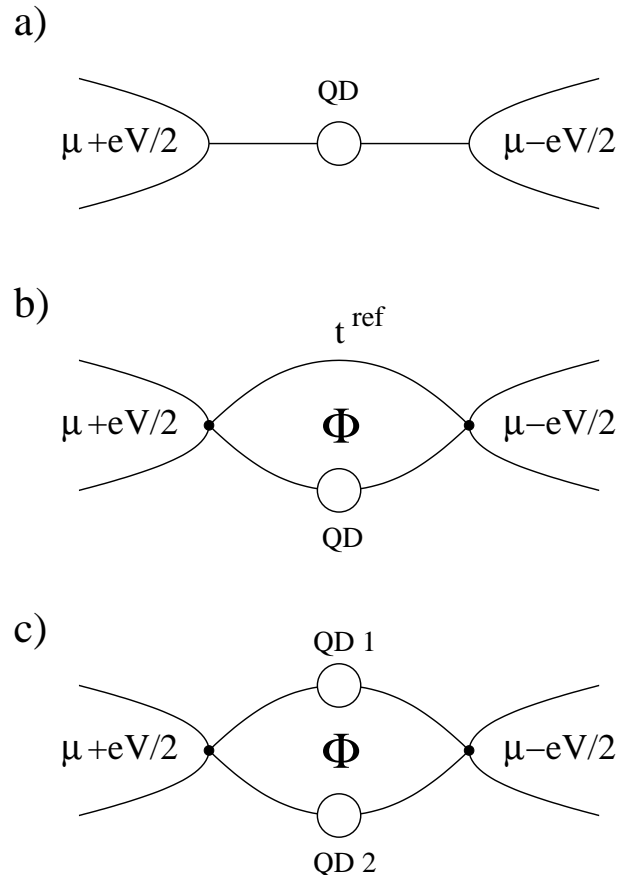


FIG. 2. Transport through a QD and AB interferometers with either one or two QDs.

We develop a simple physical picture to underline the essential physics involved in the predicted interaction-induced asymmetry of the interference signal around resonance peaks. All statements made in this section will be backed up by strict calculations for the AB interferometers in the subsequent sections. Furthermore, we give an explicit example of how the single-particle formalism breaks down in the presence of Coulomb interaction.

We consider a single-level QD with level energy  $\epsilon$ , measured from the Fermi energy of the leads. The Hamiltonian

$$H^{\text{dot}} = H_L + H_R + H_D + H_T \quad (2.1)$$

contains a part describing noninteracting electrons in the left and right leads,

$$H_r = \sum_{k\sigma} \epsilon_{kr} a_{k\sigma r}^\dagger a_{k\sigma r} \quad (2.2)$$

with  $r = L/R$ . The isolated dot is described by

$$H_D = \epsilon \sum_{\sigma} n_{\sigma} + U n_{\uparrow} n_{\downarrow}, \quad (2.3)$$

where  $n_{\sigma} = c_{\sigma}^\dagger c_{\sigma}$  counts the number of electrons with spin  $\sigma$ . The energy of the dot level  $\epsilon$  can be varied by an applied gate voltage. The electron-electron interaction is accounted for by the charging energy penalty  $U = 2(e^2/(2C))$  for double occupancy, where  $C$  is the effective capacitance of the QD. To keep the discussion simple we choose the generic limits  $U = 0$  for the noninteracting case and  $U = \infty$  for an interacting QD. We stress that the pursuant analysis, and in particular our qualitative conclusions, are applicable to the case of finite  $U$  as well. Tunneling between the QD and the leads is modeled by

$$H_T = \sum_{k\sigma r} (t_r a_{k\sigma r}^\dagger c_{\sigma} + \text{H.c.}). \quad (2.4)$$

(We neglect the energy dependence of the tunnel matrix elements  $t_{L/R}$ ). Due to tunneling the dot level acquires a finite linewidth  $\Gamma = \Gamma_L + \Gamma_R$  with

$$\Gamma_{L/R} = 2\pi |t_{L/R}|^2 N_{L/R}, \quad (2.5)$$

where  $N_{L/R}$  is the density of states in the corresponding lead.

For the sake of developing physical insight, we consider an off-resonance scenario, i.e., the gate voltage is tuned in such a way that  $|\epsilon| \gg k_B T, \Gamma$ . In this regime (and as long as the temperature is higher than the Kondo temperature), transport is dominated by second-order processes in  $\Gamma$ , which are usually called cotunneling.<sup>35,36</sup> Furthermore, we assume an infinite large charging energy  $U = \infty$ . Figure 3 shows all processes (second order in  $\Gamma$ ) which contribute to the current from left to right in which the incoming electron has spin up. Similarly, there are processes in which the incoming electron has

spin down. They will introduce a trivial factor of 2 to the final expressions for the current. The three possible second-order processes are

- (a) a (spin-up) electron enters the QD, leading to a virtual occupancy, and then leaves it to the other side.
- (b) a (spin-up) electron leaves the QD, and an electron with the same spin enters.
- (c) a (spin-down) electron leaves the QD, and an electron with opposite spin enters.

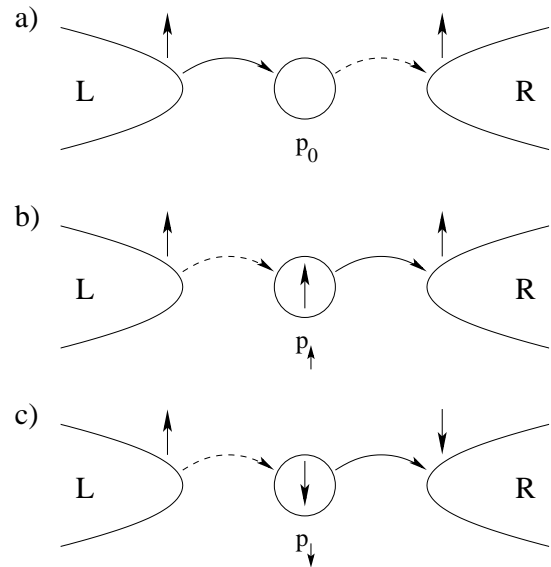


FIG. 3. Cotunneling processes for  $U = \infty$ . The solid line indicates the process that happens first, the dashed line the process that occurs afterwards. Double occupancy of the QD in the initial, intermediate, or final state is prohibited by charging energy.

Note that double occupancy of the dot (even in a virtual state) is forbidden since we have assumed  $U = \infty$ . All processes are elastic in the sense that the energy of the QD has not changed between its initial and final states. Process (c), though, is incoherent since the spin in the QD has been flipped. In other words, the traversing electron has left a trace in the “environment” (i.e., the dot). This implies that when the QD is embedded in one of the arms of an AB interferometer, one will be able to tell that an electron participating in process (c) has indeed traversed the arm with the QD (rather than the other arm). Such a process will then contribute to the total current but not to the flux-sensitive component thereof, independent of the realization of the AB interferometer. The notion that energy exchange is not necessary for dephasing,<sup>38</sup> and that the latter can take place through, e.g., a spin flip of an external degree of freedom, has been made early on.<sup>39</sup> In our case the electrons in the QD itself (and their spin) serve as the “dephasing bath”.<sup>40</sup>

Our simple picture already indicates that the physics

in adjacent Coulomb blockade valleys is qualitatively different. This is the origin of the asymmetry in the visibility discussed throughout this paper. In our model there are two possible charge states for the QD: the dot being empty,  $N = 0$ , or singly occupied,  $N = 1$ , with either spin up or down. By tuning the gate voltage (which changes the level position  $\epsilon$ ) one can drive the system away from resonance, where both states  $N = 0$  and  $N = 1$  are possible, to the Coulomb blockade valley with a fixed electron number. The latter is either  $N = 0$  or, on the other side of the resonance,  $N = 1$ . In the first case, the main contribution to the current is due to the coherent process (a) in Fig. 3. In the latter case, two processes, (b) and (c), contribute to the current but only one of them, namely (b), is coherent. We thus expect that in an AB interferometer with a single QD the AB amplitude at a gate voltage  $V_g^{(0)}$  in the  $N = 0$  valley will be twice as large as the AB amplitude at a gate voltage  $V_g^{(1)}$  in the  $N = 1$  valley. For such a comparison one needs to consider gate voltages  $V_g^{(0)}$  and  $V_g^{(1)}$  for which the flux-averaged transmission is the same. We also note that a multilevel system may offer more complex configurations, e.g., a resonance which separates a valley with all levels doubly occupied from a valley where one extra electron is added and one, three, or more levels are now singly occupied.

The transmission probabilities of electrons with energy  $\omega$  near the Fermi level of the leads can be obtained by calculating the transition rate in second-order perturbation theory and multiplying it with the probabilities  $P_\chi$  to find the system in the corresponding initial state  $\chi$ . For an incoming electron with spin up the transmission probabilities are  $P_\chi \Gamma_L \Gamma_R \text{Re}[1/(\omega - \epsilon + i0^+)^2]$  with  $\chi = 0, \uparrow, \downarrow$  for case (a), (b), and (c), respectively. Since  $P_0 + P_\uparrow + P_\downarrow = 1$  and  $P_0 + P_\sigma = 1/[1 + f(\epsilon)]$  in equilibrium, where  $f(\epsilon)$  is the Fermi function, we find for the transmission probability through the QD that  $T_\sigma^{\text{dot}}(\omega) = T_\sigma^{\text{dot,coh}}(\omega) + T_\sigma^{\text{dot,incoh}}(\omega)$  with<sup>41</sup>

$$T_\sigma^{\text{dot}}(\omega) = \text{Re} \frac{\Gamma_L \Gamma_R}{(\omega - \epsilon + i0^+)^2}, \quad (2.6)$$

$$T_\sigma^{\text{dot,coh}}(\omega) = \frac{T_\sigma^{\text{dot}}(\omega)}{1 + f(\epsilon)}. \quad (2.7)$$

In linear response the participating electrons have energies  $\omega$  that are spread by  $k_B T$  around the Fermi energy. Since we consider an off-resonance situation, we can set  $\omega \approx 0$  in Eqs. (2.6) and (2.7) and find that, while the total transmission is symmetric under  $\epsilon \rightarrow -\epsilon$ , the factor  $1/[1 + f(\epsilon)]$  ascribes an asymmetry to the coherent part.

We have argued that incoherence is induced by flipping the spin of the transferred electron, Fig. 3c. One might expect naively that such spin-flip processes may take place for noninteracting systems as well. On the other hand, in the absence of interaction, transport should be fully coherent. This puzzle is solved by the observation that in the absence of interaction,  $U = 0$ , double occupancy

of the dot is allowed and, therefore, more processes are possible. Figure 4 depicts these additional second-order processes (with an incoming spin-up electron). Spin flip takes place in Figs. 3c and 4c only. The first is hole-like while the second is particle-like (the solid line indicates the first step and the dashed line the second step of the process). Both amplitudes have the same magnitude but come with opposite signs and, hence, cancel out.

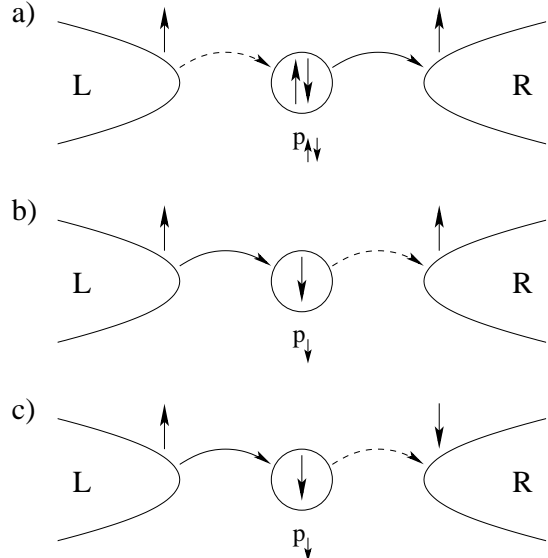


FIG. 4. Additional cotunneling processes for  $U < \infty$ . Now also double occupancy of the QD is possible.

Thus, *in the absence of Coulomb interaction* (and no coupling to an external environment) *there are no spin-flip processes, and the transmission is fully coherent*. We perform an analogous second-order perturbation calculation as above, use  $P_0 + P_\uparrow + P_\downarrow + P_{\uparrow\downarrow} = 1$ , and find that  $T_\sigma^{\text{dot}}(\omega) = T_\sigma^{\text{dot,coh}}(\omega)$  given by Eq. (2.6) without any asymmetry factor. Once  $U$  is turned on, the exact cancellation of the spin-flip processes is lost, and incoherent transmission channels induce an asymmetry of the AB signal.

As mentioned in the previous section, for noninteracting systems the transmission amplitude is determined by the retarded single-particle Green's function from the left to the right lead, and then we can easily apply the Landauer-Büttiker formalism. In our case this amplitude can be expressed as

$$t_\sigma^{\text{dot}}(\omega) = i\sqrt{\Gamma_L \Gamma_R} G_\sigma^r(\omega), \quad (2.8)$$

where the dot Green's function  $G_\sigma^r(\omega)$  is the Fourier transform of  $-i\Theta(t)\langle\{c_\sigma(t), c_\sigma^\dagger(0)\}\rangle$ . We insert the dot Green's function (for  $U = 0$  and zeroth order in  $\Gamma$ ) into Eq. (2.8) and get  $t_\sigma^{\text{dot}}(\omega) = i\sqrt{\Gamma_L \Gamma_R}/(\omega - \epsilon + i0^+)$  which yields

$$|t_\sigma^{\text{dot}}(\omega)|^2 = T_\sigma^{\text{dot}}(\omega), \quad (2.9)$$

with  $T_\sigma^{\text{dot}}(\omega)$  given by Eq. (2.6).

In the presence of interaction, however, Eq. (2.8) is no longer a good definition for the transmission amplitude. To see this we calculate the dot Green's function in the limit  $U = \infty$  and zeroth order in  $\Gamma$ . We find  $t_\sigma^{\text{dot}}(\omega) = i(P_0 + P_\uparrow)\sqrt{\Gamma_L\Gamma_R}/(\omega - \epsilon + i0^+)$  and, therefore,

$$|t_\sigma^{\text{dot}}(\omega)|^2 = \frac{T_\sigma^{\text{dot}}(\omega)}{[1 + f(\epsilon)]^2}. \quad (2.10)$$

We see that not only does  $|t_\sigma^{\text{dot}}(\omega)|^2$  not yield the total transmission Eq. (2.6) through the dot, but it differs from the coherent part of the transmission, Eq. (2.7), as well: there is no direct physical meaning of the expression  $|t_\sigma^{\text{dot}}(\omega)|^2$ .

Can we find a similar clear picture for first-order transport in  $\Gamma$ , which dominates at resonance? As long as quantum coherence is not addressed, first-order transport through QDs has been successfully described by the use of the sequential-tunneling picture or ‘‘orthodox theory’’. Tunneling rates into and out of the QD are calculated with Fermi's golden rule. They are connected to the probabilities for the dot states by a master equation, and determine the current. According to this philosophy, different tunneling processes in or out of the QD are uncorrelated since it is implicitly assumed that the electron experiences some dephasing during its stay in the QD. As a consequence the sequential-tunneling picture implies that first-order transport should be completely incoherent. This may be well justified for large QDs which are coupled to phonons or other degrees of freedom. But for the system under consideration in this paper, a single-level QD with no coupling to external baths, this is not the case. For  $U = 0$  we even expect fully coherent transport to all orders in  $\Gamma$ . As we will prove in Sec. IV by strict calculations, the sequential-tunneling picture completely misjudges the coherence of first-order transport, although it predicts the correct transmission probability through a QD. In our case, first-order transport should rather be viewed as ‘‘resonant tunneling’’ expanded up to first order than visualized as a sequence of (incoherent) sequential-tunneling processes.

### III. INTERFEROMETRY WITH A SINGLE QD

To support the results of our intuitive picture, we analyze quantitatively AB interferometers which contain a single QD, such as shown in Fig. 2b. We emphasize that all following results (except for the discussion of many levels in Sec. III E) are derived by strict calculation of the total current through the device in the presence of magnetic flux. At no point we make use of the qualitative picture outlined in the previous section. The compatibility of our calculations with the intuitive picture serves rather as a check.

Electrons emitted from the left lead have two possible ways to reach the drain on the right. They can either

go through the QD in the lower arm or choose the upper arm. We denote the transmission amplitude for the latter trajectory by  $t^{\text{ref}}$  and assume that it is independent of energy  $\omega$  and spin  $\sigma$ . The total transmission probability  $T_\sigma^{\text{tot}}(\omega)$  through this device is the sum of three parts,

$$T_\sigma^{\text{tot}}(\omega) = T_\sigma^{\text{dot}}(\omega) + T_\sigma^{\text{ref}} + T_\sigma^{\text{flux}}(\omega). \quad (3.1)$$

The terms  $T_\sigma^{\text{dot}}(\omega)$  and  $T_\sigma^{\text{ref}} = |t^{\text{ref}}|^2$  are the flux-insensitive transmissions through the QD and the reference arm, respectively. (In principle,  $T_\sigma^{\text{dot}}(\omega)$  feels the presence of the reference arm and vice versa. When low-order transmission in the couplings is considered this influence may be ignored.) Interference is described by the remaining term,  $T_\sigma^{\text{flux}}(\omega)$ , which depends on magnetic flux.

#### A. Current formula

In the first step we relate the flux-dependent nonlinear current to the dot Green's function for the closed geometry, Fig. 2b. This derivation is somewhat technical but straightforward. The central result of this part is the current in first order in  $t^{\text{ref}}$ , Eq. (3.12) [along with the zeroth-order result, Eqs. (3.9)]. The total Hamiltonian,

$$H = H^{\text{dot}} + H^{\text{ref}}, \quad (3.2)$$

consists of two parts. The first,  $H^{\text{dot}}$ , given by Eq. (2.1), describes the arm containing the QD, and the second,

$$H^{\text{ref}} = \sum_{k \in R, q \in L, \sigma} (\tilde{t} a_{k\sigma R}^\dagger a_{q\sigma L} + \text{H.c.}), \quad (3.3)$$

with  $2\pi\tilde{t}\sqrt{N_L N_R} = |t^{\text{ref}}|e^{i\varphi}$ , models the transmission through the reference arm. In general, the magnetic flux  $\Phi$  enters the phases of all three tunneling matrix elements  $t_L$ ,  $t_R$ , and  $t^{\text{ref}}$ . Above, however, we have chosen a gauge in which only  $\tilde{t}$  acquires a flux-dependent phase  $\varphi = 2\pi\Phi/\Phi_0$  but leaves  $t_L$  and  $t_R$  flux independent, and we can choose the latter to be real.

The operator for the current from the right lead is given by the time derivative of the total electron number operator  $\hat{n}_R = \sum_{k \in R, \sigma} a_{k\sigma R}^\dagger a_{k\sigma R}$  times the elementary charge  $e$ . This yields for the total current

$$I = I_R = e \frac{d\langle \hat{n}_R \rangle}{dt} = i \frac{e}{\hbar} \langle [\hat{H}, \hat{n}_R] \rangle. \quad (3.4)$$

The latter expression yields Green's functions which involve Fermi operators of the right lead and of either the left lead or the dot,

$$I_R = -\frac{e}{\hbar} \sum_{q \in L, k \in R, \sigma} \int d\omega \left[ \tilde{t} G_{qk, \sigma}^<(\omega) + \text{H.c.} \right] - \frac{e}{\hbar} \sum_{k \in R, \sigma} \int d\omega \left[ t_R G_{dk, \sigma}^<(\omega) + \text{H.c.} \right], \quad (3.5)$$

with the notations  $G_{qk,\sigma}^<(t) = i\langle a_{k\sigma R}^\dagger(0)a_{q\sigma L}(t) \rangle$  and  $G_{dk,\sigma}^<(t) = i\langle a_{k\sigma R}^\dagger(0)c_\sigma(t) \rangle$ . The indices  $q$  and  $k$  label the states in the left and right leads, respectively. The index  $d$  indicates that a dot electron operator is involved (in our simple model there is only one dot level). The other Green's functions are defined similarly,  $G_{kq,\sigma}^<(t) = i\langle a_{q\sigma L}^\dagger(0)a_{k\sigma R}(t) \rangle$  and  $G_{kd,\sigma}^<(t) = i\langle c_\sigma^\dagger(0)a_{k\sigma R}(t) \rangle$ . Note that, since the  $z$  component of the spin of the entire system is conserved (as well as the total spin), only Green's functions which are diagonal in spin space are involved.

The first (second) line of Eq. (3.5) describes electron transfer from the left (from the QD) to the right lead or vice versa. This transfer can be a direct tunneling process or a complex trajectory through the entire device. We emphasize that Eq. (3.5) is exact as long as the full Green's functions with contributions of arbitrary high order in  $t$  and  $t^{\text{ref}}$  are inserted.

Our goal is to derive a relation between the current and Green's functions involving only dot operators. To achieve this we employ the Keldysh technique and use the matrix representation

$$\mathbf{G} = \begin{pmatrix} G^r & G^< \\ 0 & G^a \end{pmatrix}, \quad (3.6)$$

where  $G^r$  and  $G^a$  are the usual retarded and advanced Green's functions, respectively.

The contribution to the total current can be classified by powers of  $t^{\text{ref}}$ . The zeroth-order term  $I_R^{(0)}$  represents the current through the QD in the absence of the reference arm and is independent of magnetic flux. The main contribution  $I_R^{(1)}$  to the flux-dependent part is first order in  $t^{\text{ref}}$ . In the spirit of a series expansion we drop in the flux-dependent part all second- or higher-order terms of  $t^{\text{ref}}$ , which is a good approximation as long as the transmission through the reference arm is small (trajectories with higher winding numbers, where an electron moves around the enclosed flux several times, are described by such higher-order terms). Transmission through the reference arm, which is at least of order  $(t^{\text{ref}})^2$ , is not considered in this subsection.

We start with the zeroth-order term,  $I_R^{(0)}$ . Only the second line of Eq. (3.5) has to be included since the first line explicitly contains  $\tilde{t}$ . Since the electrons in the leads are noninteracting, we get the Dyson-like equation  $\mathbf{G}_{dk,\sigma}^{(0)}(\omega) = \mathbf{G}_\sigma^{(0)}(\omega)t_R\mathbf{g}_{k,\sigma}(\omega)$ , where  $G_\sigma^<(t) = i\langle c_\sigma^\dagger c_\sigma(t) \rangle$  is the Green's functions of the dot, and  $g_{k,\sigma}^< = i\langle a_{k\sigma R}^\dagger a_{k\sigma R}(t) \rangle$  for the leads, and the retarded and advanced Green's functions are defined similarly. We do the analog for  $G_{kd,\sigma}^<$ . For the (noninteracting) leads we make use of  $g_{k,\sigma}^<(\omega) = 2\pi i f_R(\omega)\delta(\omega - \epsilon_k)$ ,  $g_{k,\sigma}^r(\omega) = 1/(\omega - \epsilon_k + i0^+)$ , and  $g_{k,\sigma}^a(\omega) = \left(g_{k,\sigma}^r(\omega)\right)^*$ .

We obtain then

$$I_R^{(0)} = -\frac{ie}{h}\Gamma_R \sum_\sigma \int d\omega \left[ G_\sigma^<^{(0)} + f_R \left( G_\sigma^{r(0)} - G_\sigma^{a(0)} \right) \right]. \quad (3.7)$$

As a check we verify that in equilibrium,  $V = 0$ , the relation  $G^<(\omega) + f(\omega)[G^r(\omega) - G^a(\omega)] = 0$  guarantees that no current is flowing,  $I_R = 0$ .

It is straightforward to derive an analogous expression for  $I_L^{(0)}$  for the left lead. The total current must be conserved,  $I_L^{(0)} + I_R^{(0)} = 0$ . Even more, the current must be conserved for each spin separately. This yields the condition

$$0 = \int d\omega \left[ G_\sigma^<^{(0)} + \frac{\Gamma_L f_L + \Gamma_R f_R}{\Gamma_L + \Gamma_R} \left( G_\sigma^{r(0)} - G_\sigma^{a(0)} \right) \right] \quad (3.8)$$

for the integral (but not for each energy  $\omega$  separately). Due to current conservation we can write  $I_R = (\Gamma_L I_R - \Gamma_R I_L)/(\Gamma_L + \Gamma_R)$  and find the well-known result for the current through a QD (in the absence of a reference arm),

$$I_R^{(0)} = -\frac{2e}{h} \frac{\Gamma_L \Gamma_R}{\Gamma_L + \Gamma_R} \sum_\sigma \int d\omega \text{Im} G_\sigma^{r(0)}(f_L - f_R), \quad (3.9)$$

and  $A_\sigma(\omega) = -(1/\pi) \text{Im} G_\sigma^r(\omega)$  is the spectral density.

We now turn to the flux-dependent term  $I_R^{(1)}$ . Similarly to the above, we can make use of Dyson-like equations. We get a contribution from the first line of Eq. (3.5) and use  $\mathbf{G}_{qk,\sigma}^{(0)}(\omega) = \mathbf{g}_{q,\sigma}(\omega)t_L\mathbf{G}_\sigma^{(0)}(\omega)t_R\mathbf{g}_{k,\sigma}(\omega)$ . For the contributions of the second line of Eq. (3.5) we make use of  $\mathbf{G}_{dk,\sigma}^{(1)}(\omega) = \mathbf{G}_\sigma^{(0)}(\omega)t_L\mathbf{g}_{q,\sigma}(\omega)\tilde{t}\mathbf{g}_{k,\sigma}(\omega) + \mathbf{G}_\sigma^{(1)}(\omega)t_R\mathbf{g}_{k,\sigma}(\omega)$ . After collecting all terms and employing the relation  $4\pi^2\tilde{t}t_R t_L N_L N_R = \sqrt{\Gamma_L \Gamma_R}|t^{\text{ref}}|e^{i\varphi}$  we get<sup>42</sup>

$$I_R^{(1)} = \frac{e}{h} \sqrt{\Gamma_L \Gamma_R} |t^{\text{ref}}| \sum_\sigma \int d\omega \left[ \cos \varphi \left( G_\sigma^{r(0)} + G_\sigma^{a(0)} \right) (f_L - f_R) + i \sin \varphi \left( G_\sigma^<^{(0)} + f_L \left( G_\sigma^{r(0)} - G_\sigma^{a(0)} \right) \right) - \frac{ie}{h} \Gamma_R \sum_\sigma \int d\omega \left[ G_\sigma^<^{(1)} + f_R \left( G_\sigma^{r(1)} - G_\sigma^{a(1)} \right) \right] \right]. \quad (3.10)$$

Again, we can check that due to the equilibrium relation  $G^<(\omega) + f(\omega)[G^r(\omega) - G^a(\omega)] = 0$  the current vanishes at zero bias voltage. The current conservation (for each spin) in first order in  $t^{\text{ref}}$  is equivalent to

$$\frac{\sqrt{\Gamma_L \Gamma_R}}{\Gamma_L + \Gamma_R} |t^{\text{ref}}| \sin \varphi \int d\omega \left( G_\sigma^{r(0)} - G_\sigma^{a(0)} \right) (f_L - f_R) = \int d\omega \left[ G_\sigma^<^{(1)} + \frac{\Gamma_L f_L + \Gamma_R f_R}{\Gamma_L + \Gamma_R} \left( G_\sigma^{r(1)} - G_\sigma^{a(1)} \right) \right]. \quad (3.11)$$

Note that to ensure current conservation, Green's functions of higher order in  $t^{\text{ref}}$  are important since the first

line of Eq. (3.11) alone is in general nonzero (comparison with Eq. (3.9) shows that it is even proportional to the current  $I^{(0)}$  in zeroth order). This means that for a systematic and consistent description the influence of the reference arm on the QD has to be taken into account properly. It is, in general, not sufficient to treat the Green's function of the QD independent of the surrounding environment in the device. One has, therefore, to check carefully in each case up to what extent the interference signal probes the properties of the QD.

We use  $I_R = (\Gamma_L I_R - \Gamma_R I_L)/(\Gamma_L + \Gamma_R)$  and the current conservation in zeroth order, Eq. (3.8), to get

$$I_R^{(1)} = \frac{2e}{h} \sqrt{\Gamma_L \Gamma_R} |t^{\text{ref}}| \cos \varphi \sum_{\sigma} \int d\omega \operatorname{Re} G_{\sigma}^{r(0)}(f_L - f_R) - \frac{2e}{h} \frac{\Gamma_L \Gamma_R}{\Gamma_R + \Gamma_L} \sum_{\sigma} \int d\omega \operatorname{Im} G_{\sigma}^{r(1)}(f_L - f_R). \quad (3.12)$$

This is the central result of the present derivation. Again, we emphasize that the influence of the reference arm on the QD plays a role (it shows up in the Green's functions which are of first order in  $t^{\text{ref}}$ ). Furthermore, we remark that the Green's functions  $G^{(0)}$  and  $G^{(1)}$  include multiple tunneling between QD and leads, i.e., they include contributions from arbitrary high order in  $t$  (the superscripts (0) and (1) only labels the order in  $t^{\text{ref}}$ ).

### B. Linear-response regime

In the linear-response regime, we replace  $f_L(\omega) - f_R(\omega) \rightarrow -eVf'(\omega)$  in Eq. (3.12) and take the Green's functions at equilibrium. The first line in Eq. (3.12) is obviously symmetric under reversal of magnetic flux,  $\varphi \rightarrow -\varphi$ . Moreover, in equilibrium also the Green's functions  $G^{(1)}$  have this property.<sup>43</sup> This establishes phase locking in linear response, as expected for a two-terminal device.

The situation simplifies further if we concentrate on the dominant contribution to the flux-dependent linear conductance, which is of first order in  $\Gamma$  and first order in  $t^{\text{ref}}$ . In this case the second line of Eq. (3.12) drops out (since there is a prefactor of order  $\Gamma$  and the equilibrium Green's function  $G^{(1)}$  in zeroth order in  $\Gamma$  vanishes). The connection to the transmission is established by Eq. (1.1). We obtain

$$T_{\sigma}^{\text{flux}}(\omega) = 2\sqrt{\Gamma_L \Gamma_R} |t^{\text{ref}}| \cos \varphi \operatorname{Re} G_{\sigma}^{r(0)}(\omega), \quad (3.13)$$

and realize that up to the given order the influence of the reference arm on the QD does not matter for the transport properties.

For comparison we cite the result for a system with an open geometry,<sup>14</sup>

$$T_{\sigma}^{\text{flux,open}}(\omega) = 2\sqrt{\Gamma_L \Gamma_R} |t^{\text{ref}}| \operatorname{Re} \left[ e^{-i\theta} G_{\sigma}^{r(0)}(\omega) \right], \quad (3.14)$$

with  $\theta = \varphi + \Delta\theta$ , where  $\Delta\theta$  is determined by the specifics of the interferometer. The two expressions Eqs. (3.13) and (3.14) look very similar. One should keep in mind, though, that in higher orders in  $\Gamma$  or in nonlinear response an additional term, which originates from the second line of Eq. (3.12) enters, while for the derivation of Eq. (3.14) one considers a special case of open geometry where the reference arm has no effect on the QD's properties.

The transmission Eq. (3.13) is always extremal at  $\varphi = 0$ . Such a "phase locking" does not take place in the open-geometry setup: the AB phase at which the transmission is extremal can be continuously varied by tuning the energy of the dot level via a gate electrode.

### C. Probing the total spin of an interacting QD

In linear response and lowest order in  $t^{\text{ref}}$  and  $\Gamma$  we get  $G_{\sigma}^{r(0)}(\omega) = 1/(\omega - \epsilon + i0^+)$  for  $U = 0$  and, according to Eq. (3.13), the amplitude of the flux-dependent linear conductance is symmetric around  $\epsilon = 0$ . This is consistent with our intuitive picture, since in the absence of spin-flip processes no incoherent channels are involved on either side of the resonance.

This changes when electron-electron interaction in the QD is important. For  $U = \infty$  the retarded Green's function

$$G_{\sigma}^{r(0)}(\omega) = \frac{1}{1 + f(\epsilon)} \cdot \frac{1}{\omega - \epsilon + i0^+} \quad (3.15)$$

acquires a prefactor  $P_0 + P_{\sigma} = 1/[1 + f(\epsilon)]$  in linear response and lowest order in  $t^{\text{ref}}$  and  $\Gamma$ . This prefactor indicates an "interaction-induced" asymmetry associated with spin-flip processes.

For illustration we show in Fig. 5 the flux-dependent linear conductance as a function of the level position  $\epsilon$  for a fixed value  $\varphi = 0$ . In order to obtain the flux dependence, the result simply has to be multiplied by  $\cos \varphi$ . At  $\epsilon = 0$  the AB oscillations vanish. [Note that we consider here only the first harmonic Eq. (3.12). Higher harmonics survive, an effect known as frequency doubling.] In the absence of interaction,  $U = 0$ , the amplitude of the AB signal is symmetric around that point, while for  $U = \infty$  clear asymmetry is predicted. When the QD is most likely filled up with one electron, the total spin of the QD is 1/2 and spin-flip processes reduce the interference signal. On the other side of the resonance,  $\epsilon > 0$ , the QD is most likely empty. The total spin is 0 and the AB oscillations are by a factor of 2 larger than for  $\epsilon < 0$ .



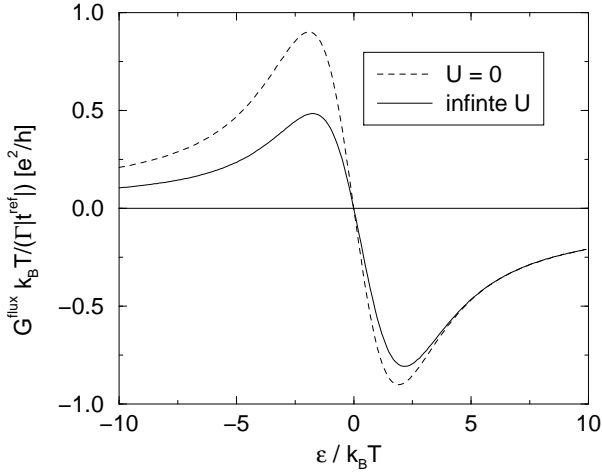


FIG. 5. Interference signal for AB interferometer with a single QD. Asymmetry in the magnitude of the signal appears for nonzero  $U$ . Plotted is the flux-dependent part of the conductance, normalized by  $|t^{\text{ref}}|\Gamma/(k_B T)$ , in units of  $e^2/h$ .

It is well known that due to the Kondo effect the transport through a QD increases at low temperature for  $\epsilon < 0$  but not for  $\epsilon > 0$ . Therefore, the Kondo effect reveals the same information as our procedure. We note, however, that the Kondo effect occurs under much more stringent experimental conditions, namely, strong coupling of the QD to the leads and low temperatures (in comparison to the Kondo temperature). In contrast, our approach to detect the spin of the QD works in the experimentally easier accessible regime of weak coupling and high temperatures.

#### D. Coherence of non-spin-flip cotunneling

As has been outlined in the introduction we use the following procedure to investigate the coherence of cotunneling. We tune the system away from resonance, where transport through the QD is dominated by the usual cotunneling processes. We then try to find an AB setup such that the total conductance *vanishes* once a reference arm is *added*, i.e., we look for complete destructive interference of the coherent channels. (The existence of AB oscillations alone only proves *partial* coherence.) We remind ourselves that the transport through the AB interferometer probes many channels, characterized by energy  $\omega$  and spin  $\sigma$ , simultaneously. Zero transport can only be achieved when *all* channels show destructive interference at the same time. To achieve this we want to adjust the magnitude of the amplitude  $t^{\text{ref}}$  for transmission through the reference arm such that  $T_\sigma^{\text{dot}}(\omega) = T_\sigma^{\text{ref}}$  for *all* contributing energies.

Cotunneling is the dominant transport channel when  $|\epsilon| \gg \Gamma, k_B T$  applies. In this regime, the linear-response conductance through the QD in the absence of the reference arm is

$$\left. \frac{\partial I^{\text{dot}}}{\partial V} \right|_{V=0} = \frac{2e^2}{h} \frac{\Gamma_L \Gamma_R}{\epsilon^2} \quad (3.16)$$

for both  $U = 0$  and  $U = \infty$ . Cotunneling through the QD is of second order in  $\Gamma$ . The conductance through the reference arm in the absence of the QD is

$$\left. \frac{\partial I^{\text{ref}}}{\partial V} \right|_{V=0} = \frac{2e^2}{h} |t^{\text{ref}}|^2. \quad (3.17)$$

We now make the adjustment  $|t^{\text{ref}}| = \sqrt{\Gamma_L \Gamma_R}/|\epsilon|$ , i.e.,  $|t^{\text{ref}}|$  is of order  $\Gamma$ . Therefore, the Green's function which enters the flux-dependent transmission Eq. (3.13) is of zeroth order in  $\Gamma$  and  $t^{\text{ref}}$ , i.e., the influence of the reference arm on the QD is not probed under the present conditions. We find for the total conductance

$$\left. \frac{\partial I^{\text{tot}}}{\partial V} \right|_{V=0} = \frac{4e^2}{h} \frac{\Gamma_L \Gamma_R}{\epsilon^2} \left[ 1 - \frac{\epsilon}{|\epsilon|} \cos \varphi \right] \quad (3.18)$$

for the noninteracting case and

$$\left. \frac{\partial I^{\text{tot}}}{\partial V} \right|_{V=0} = 4 \frac{e^2}{h} \frac{\Gamma_L \Gamma_R}{\epsilon^2} \left[ 1 - \frac{\epsilon}{|\epsilon|} \frac{\cos \varphi}{1 + f(\epsilon)} \right] \quad (3.19)$$

for  $U = \infty$ . This shows that cotunneling in the noninteracting case is fully coherent. In the interacting case spin-flip processes are present which spoils coherence. This is described by the asymmetry factor  $1/[1 + f(\epsilon)]$ , in accordance with our intuitive picture.

We conclude that an AB interferometer containing a single QD is suitable to prove coherence of non-spin-flip cotunneling through the QD.

#### E. Many levels

In the model we discussed so far, the spacing  $\Delta$  of the dot levels was assumed to be larger than the charging energy and the energy scale provided by the temperature, the intrinsic linewidth or the voltage bias, so that only one dot level participates in transport. We found that the ratio of the number of coherent to the total number of cotunneling channels was 1 or 1/2 in the valley where the electron number of the dot is even or odd, respectively, giving rise to an observable asymmetry in the interference signal. The resulting sequence of asymmetric AB oscillations is shown schematically in Fig. 6. For a continuum of levels, such as in metallic quantum dots,  $\Delta = 0$ , incoherent cotunneling dominates and we expect little asymmetry. Dephasing due to electron-electron interactions in the dot is beyond the scope of the present analysis, but is known<sup>44</sup> to be inefficient.

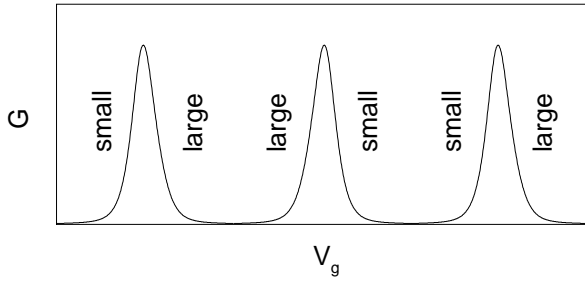


FIG. 6. Sequence of asymmetry of AB oscillations in the Coulomb blockade regime. The solid line depicts schematically the conductance oscillations vs. the gate voltage  $V_g$ , and shows the Coulomb peaks. Regions of small and large AB amplitudes are indicated, showing the asymmetry between two adjacent Coulomb blockade valleys (“large” corresponds to a valley with a total spin 0, while “small” corresponds to an  $S = 1/2$  valley).

To investigate how the crossover occurs we count the number of coherent and incoherent cotunneling channels for a system with arbitrary level spacing  $\Delta$ . We examine four different situations. In all of them the level energy  $\epsilon$  is tuned away from resonance,  $k_B T, \Gamma \ll |\epsilon| < U/2$ . The four situations arise due to the combination of being in a valley which corresponds to an even or odd electron number of the dot and being on either side of the resonance, i.e., only particle-like or hole-like cotunneling is considered.

When the level spacing  $\Delta$  becomes comparable to  $|\epsilon|$  the number of dot levels involved in transport is increased from 1 to  $N \sim 2|\epsilon|/\Delta + 1$  (each of them is spin degenerate). As long as  $\Delta \gg k_B T$ , no inelastic cotunneling process takes place which changes the energy of the QD. Incoherence occurs only due to spin flip. In the “even” valley all channels are coherent while in the “odd” valley 1 out of  $N + 1$  corresponds to spin flip and is, therefore, incoherent (the total number of channels is always the same). The relative asymmetry around the resonance peaks is  $N/(N+1)$  and vanishes for large  $N$ , i.e.,  $\Delta \ll |\epsilon|$ .

Now we reduce  $\Delta$  further such that  $\Delta \ll k_B T$ . The number of levels within the range defined by temperature is  $M \sim 2k_B T/\Delta \gg 1$  (each of them is spin degenerate). For a simple estimate we assume that all single-particle states within the energy range  $\pm k_B T$  around the Fermi energy in the leads are occupied with probability 1/2, all states above that range are empty, and all states below are filled. For the single-particle states in the QD we do the same. Let  $\delta$  be the level spacing in the leads with  $\delta \ll \Delta$ . The number of coherent channels (times the probabilities that the corresponding states are empty or occupied) is then

$$\frac{\Delta}{\delta} \cdot \frac{NM}{2}. \quad (3.20)$$

Next, we count the number of incoherent channels where an excitation of energy  $E$  is left on the QD ( $E$  is an integer multiple of  $\Delta$ ). For  $E > 0$  and given the

spin of the incoming and outgoing electron there are  $[M + 3(E/\Delta)]/4$  combinations to leave this excitation on the QD (where the probabilities to find the corresponding state empty or filled are already included). For  $E < 0$  (i.e., energy is pulled out of the QD) we have  $[M + (E/\Delta)]/4$  combinations. Energy conservation requires that the energy stored in the QD is pulled out of the leads and vice versa. An analogous consideration yields for  $E > 0$  (energy pulled out of the leads)  $(\Delta/\delta)[M + (E/\Delta)]/4$  combinations and for  $E < 0$  we get  $(\Delta/\delta)[M + 3(E/\Delta)]/4$ . In total we find, therefore,

$$\frac{1}{2} \cdot \frac{\Delta}{\delta} \cdot \sum_{n=1}^M (M + 3n)(M + n) = 2 \frac{\Delta}{\delta} [M^3 + \mathcal{O}(M^2)] \quad (3.21)$$

channels with either  $E > 0$  or  $E < 0$  (a multiplication factor of 4 was introduced to account for the spin of the incoming and outgoing electrons). The number of incoherent channels with  $E = 0$  (and spin flip) is of the order  $(\Delta/\delta)M^2$  and can be neglected.

The ratio of the number of coherent channels (for  $N \gg M \gg 1$ ) to the total number of transmission channels is  $N/(N + 4M^2)$ . As a consequence the coherent contribution vanishes for  $k_B T \gg \sqrt{|\epsilon|\Delta/8}$  or  $8(k_B T)^2/|\epsilon| \gg \Delta$ .

In summary, by reducing the dot level spacing  $\Delta$  we go through three different regimes:

- (i)  $\Delta \gg |\epsilon|$ : the asymmetry due to spin-flip cotunneling is as large as possible;
- (ii)  $|\epsilon| \gg \Delta \gg 8(k_B T)^2/|\epsilon|$ : the asymmetry vanishes but transport is dominated by coherent channels;
- (iii)  $8(k_B T)^2/|\epsilon| \gg \Delta$ : transport is dominated by incoherent channels.

## F. First-order transport

The discussion so far covered cotunneling, which dominates away from resonance. Let us now turn to the regime  $k_B T \gg \Gamma, |\epsilon|$ , where the dot level is near resonance and transmission is dominated by first-order transport in  $\Gamma$ . Can we tune the single-dot AB interferometer in such a way that full destructive interference is achieved for all those first-order transport channels that are coherent? The energy spread of electrons going through the reference arm is  $k_B T$ , while the width of the resonance through the QD is  $\Gamma$ . Hence, the temperature has to be on the one hand larger than  $\Gamma$  in order to be in the regime where first-order transport dominates, yet, on the other hand, it has to be smaller than  $\Gamma$  to allow for a destructive interference of *all* energy components simultaneously. To circumvent this problem, we consider a two-terminal AB interferometer with two QDs, one in each arm, see Fig. 2c.

#### IV. INTERFEROMETRY WITH TWO QDS

The conceptual difficulty to address first-order transport in a single-dot AB interferometer is that the temperature has to be on the one hand large, yet, on the other hand, it has to be small to allow for a destructive interference of all energy components simultaneously. As we will show in this section, this difficulty will not arise in AB interferometers which contain *two* QDs, one in each arm, see Fig. 2c. This is due to the fact that the resonance of width  $\Gamma$  of each QD filters out a small fraction of the incoming electrons in both arms, even at high temperature, and we will find that fully destructive interference (in the absence of interaction) is feasible. For interacting QDs we find again an asymmetry factor which makes it possible to distinguish on which side of the resonance the adjacent Coulomb blockade valley has an even or odd number of electrons.

Geometries similar to the two-dot AB interferometer have been investigated theoretically in the literature. Resonant tunneling (in the absence of interaction)<sup>45</sup> and cotunneling<sup>1,13</sup> have been studied in this geometry. Furthermore, a numerical renormalization-group analysis has been performed<sup>8</sup> where, by construction, only equilibrium properties of the dot were included. Spectral properties of such a double-dot system, or equivalently a two-level dot, have been addressed.<sup>17,46</sup> Recently, also experimental realization of a two-dot AB setup has been reported.<sup>12,18</sup>

##### A. General current formula

The total Hamiltonian

$$H = H^{\text{dot},1} + H^{\text{dot},2} \quad (4.1)$$

is the sum of two parts.<sup>47</sup> Each of them describe a QD coupled to (the same) reservoirs and has the structure of Eq. (2.1). We choose a completely symmetric geometry, and we assume  $k_B T \gg \Gamma$ ,  $|\epsilon_1|, |\epsilon_2|$  as well as  $\Gamma \gg |\epsilon_1 - \epsilon_2|$ , where  $\epsilon_{1,2}$  is the energy of the level in QD 1 and 2. In this regime lowest-order transport dominates, and we can set  $\epsilon = \epsilon_1 = \epsilon_2$ . To model the enclosed flux we attach a phase factor  $e^{i\varphi/4}$  to the tunnel matrix elements  $t_{R,\text{dot}1}$  and  $t_{L,\text{dot}2}$ , and  $e^{-i\varphi/4}$  to  $t_{L,\text{dot}1}$  and  $t_{R,\text{dot}2}$ . This symmetric flux dependence of the tunnel matrix elements can be achieved choosing a corresponding gauge.

The system is equivalent to a single QD with two levels (each of them spin degenerate) with  $\varphi$ -dependent tunnel matrix elements. To write the total current in a compact way we employ a  $2 \times 2$  matrix notation to account for the two QDs and get<sup>33</sup>

$$I^{\text{tot}} = \frac{ie}{2\hbar} \int d\omega \mathbf{tr} \left\{ [\Gamma^L f_L - \Gamma^R f_R] \mathbf{G}_\sigma^> + [\Gamma^L(1 - f_L) - \Gamma^R(1 - f_R)] \mathbf{G}_\sigma^< \right\} \quad (4.2)$$

with  $\Gamma^L = \frac{\Gamma}{2} \begin{pmatrix} 1 & e^{+i\varphi/2} \\ e^{-i\varphi/2} & 1 \end{pmatrix} \delta_{\sigma\sigma'}$  and  $\Gamma^R = (\Gamma^L)^*$ .

The trace has to be performed over both the spin degrees of freedom and the  $2 \times 2$  matrices. We get the general and exact result

$$I = \frac{ie}{2\hbar} \Gamma \sum_\sigma \int d\omega \left[ (G_{11,\sigma}^> - G_{11,\sigma}^< + G_{22,\sigma}^> - G_{22,\sigma}^<) (f_L - f_R) + \cos \frac{\varphi}{2} (G_{12,\sigma}^> - G_{12,\sigma}^< + G_{21,\sigma}^> - G_{21,\sigma}^<) (f_L - f_R) - 2i \sin \frac{\varphi}{2} \left( \frac{f_L + f_R}{2} \right) (G_{12,\sigma}^> - G_{21,\sigma}^>) - 2i \sin \frac{\varphi}{2} \left( 1 - \frac{f_L + f_R}{2} \right) (G_{12,\sigma}^< - G_{21,\sigma}^<) \right] \quad (4.3)$$

with the full Green's functions which includes multiple tunneling through the entire device. The indices 1 and 2 label the respective QD. Note that even the diagonal terms  $G_{11,\sigma}$  and  $G_{22,\sigma}$  are *not* the Green's functions of QD 1 and 2 in the absence of the other one. Instead, they have to be calculated in the presence of the entire geometry.

##### B. First-order transport in linear response

To address the lowest-order contribution to transport we expand Eq. (4.3) up to first order in  $\Gamma$ , i.e., only Green's functions in zeroth order are involved. The off-diagonal terms are connected by  $G_{12,\sigma}^{>(0)}(\omega) = G_{12,\sigma}^{<(0)}(\omega) = 2\pi i P_{2\sigma}^1 \delta(\omega - \epsilon)$  to the stationary off-diagonal density-matrix elements  $P_{2\sigma}^1 = \langle |2\sigma\rangle \langle 1\sigma| \rangle$  in zeroth order in  $\Gamma$ . In equilibrium (and zeroth order in  $\Gamma$ ) the density matrix is diagonal, with the probabilities determined by Boltzmann weights, and all off-diagonal matrix elements vanish. In the first and second line of Eq. (4.3), only equilibrium Green's functions are involved in linear-response transport. As a consequence, the second line of Eq. (4.3) does not contribute at all (in linear response and first order in  $\Gamma$ ). In the third and fourth line, however, *non-equilibrium Green's functions enter even in the linear-response regime*. We obtain

$$\frac{\partial I^{\text{tot}}}{\partial V} \Big|_{V=0} = \frac{2e^2}{\hbar} \Gamma \sum_\sigma \int d\omega \left\{ \text{Im} G_{11,\sigma}^{r(0)}(\omega) f'(\omega) + \sin \frac{\varphi}{2} f(\omega) \frac{\partial G_{12,\sigma}^{>(0)}}{\partial(eV)} + \sin \frac{\varphi}{2} [1 - f(\omega)] \frac{\partial G_{12,\sigma}^{<(0)}}{\partial(eV)} \right\}. \quad (4.4)$$

Here, we have used the fact that the contributions involving  $\text{Im} G_{22,\sigma}^{r(0)}(\omega)$ ,  $G_{21,\sigma}^{<(0)}(\omega)$ , and  $G_{21,\sigma}^{>(0)}(\omega)$  amount to an overall factor 2. For the first term in Eq. (4.4) we use  $-(1/\pi) \text{Im} G_{11,\sigma}^{r(0)}(\omega) = \delta(\omega - \epsilon)$  for  $U = 0$  and

$-(1/\pi) \text{Im} G_{11,\sigma}^{r(0)}(\omega) = \delta(\omega - \epsilon)/[1 + f(\epsilon)]$  for  $U = \infty$ . This term is flux independent and is twice the conductance through one QD in the absence of the other one. Interference effects are accounted for by the second and third terms. To determine the off-diagonal density-matrix element  $P_{2\sigma}^{1\sigma}$  we use the real-time transport theory developed in Refs. 29 and 34 and solve a generalized master equation. The analysis, presented in Appendix B, employs diagrams of the type used in Appendix A. We find the result (for zeroth order in  $\Gamma$  and  $V = 0$ )

$$\frac{\partial P_{2\sigma}^{1\sigma}}{\partial(eV)} = -\frac{i}{2} f'(\epsilon) \sin(\varphi/2) \quad (4.5)$$

in the absence of interaction and

$$\frac{\partial P_{2\sigma}^{1\sigma}}{\partial(eV)} = -\frac{i}{2} \frac{f'(\epsilon)}{[1 + f(\epsilon)]^3} \sin(\varphi/2) \quad (4.6)$$

for  $U = \infty$ . As a consequence, in the absence of an AB flux, only equilibrium Green's functions enter Eq. (4.4). It is crucial, however, that in the presence of the flux, nonequilibrium properties of the Green's functions are involved even for the linear-response regime.

Collecting all terms we find for the noninteracting case

$$\left. \frac{\partial I^{\text{tot}}}{\partial V} \right|_{V=0} = 2 \left. \frac{\partial I^{\text{dot}}}{\partial V} \right|_{V=0} \times [1 - \sin^2(\varphi/2)] \quad (4.7)$$

with  $(\partial I^{\text{dot}}/\partial V)|_{V=0} = -(\pi e^2/h)\Gamma f'(\epsilon)$  being the conductance through a single QD. At  $\varphi = \pm\pi, \pm3\pi, \dots$ , the total current vanishes (up to a small correction of order  $|\epsilon_1 - \epsilon_2|/\Gamma$ , which is not considered here), indicating that lowest-order transport is fully coherent. In fact it has been shown<sup>17</sup> that in this case, the system can be mapped onto a model with two levels, where each level is coupled to one of the leads only. As a consequence, in the absence of any interaction, there is no way to transfer any electron from one lead to the other. This completely contrasts the picture of sequential tunneling which predicts incoherent transmission. In the absence of interaction, however, the transport should be fully coherent. For the simple limit  $U = 0$ , we can rederive Eq. (4.7) by using the Landauer-Büttiker approach, determining the dot Green's function by equations of motion, and expanding the result up to first order in  $\Gamma$ . This is done in Appendix C. The sequential-tunneling picture is highly misleading in this context. We should rather view the transport as resonant tunneling but expanded up to lowest order in  $\Gamma$ .

In the presence of interaction we obtain

$$\left. \frac{\partial I^{\text{tot}}}{\partial V} \right|_{V=0} = 2 \left. \frac{\partial I^{\text{dot}}}{\partial V} \right|_{V=0} \times \left[ 1 - \frac{\sin^2(\varphi/2)}{[1 + f(\epsilon)]^2} \right] \quad (4.8)$$

with  $(\partial I^{\text{dot}}/\partial V)|_{V=0} = -(\pi e^2/h)\Gamma f'(\epsilon)/[1 + f(\epsilon)]$ .

We point out that the maximal total conductance (which is reached at  $\varphi = 0, \pm 2\pi, \pm 4\pi, \dots$ ) is the sum of the conductances through the QDs taken apart. There is

no extra factor 2 familiar from constructive interference, which takes place away from resonance when transmission is small. To understand this we remark that for  $\varphi = 0$  only the symmetric combination of the dot levels are coupled to the leads while the antisymmetric one is not (this holds for degenerate levels which are symmetrically coupled to the leads). At  $U = 0$  the model is, therefore, equivalent to a system with one level but tunnel matrix elements which are  $\sqrt{2}$  times the original ones. As a consequence, in first order in  $\Gamma$  (which is second order in the tunnel matrix elements) the total conductance is twice the conductance through one arm of the interferometer in the absence of the other one.

The factor  $1/[1 + f(\epsilon)]^2$  yields an interaction-induced asymmetry in the ratio of coherent to total transport around a conductance peak. This factor can be easily understood in the following way. Consider the situation where the incoming electron has spin up. Interference is possible if we start with both QDs being empty, one QD empty and the other one filled with spin up, or both QDs filled with spin up. For all other starting configurations one would be able to tell afterwards which way the transferred electron has taken. The corresponding contributions are not subject to interference. Summing up the probabilities for the four situations which allow for interference we find (at  $V = 0$ ) the factor  $1/[1 + f(\epsilon)]^2$ .

The effect of the interaction-induced asymmetry factor is illustrated in Fig. 7.

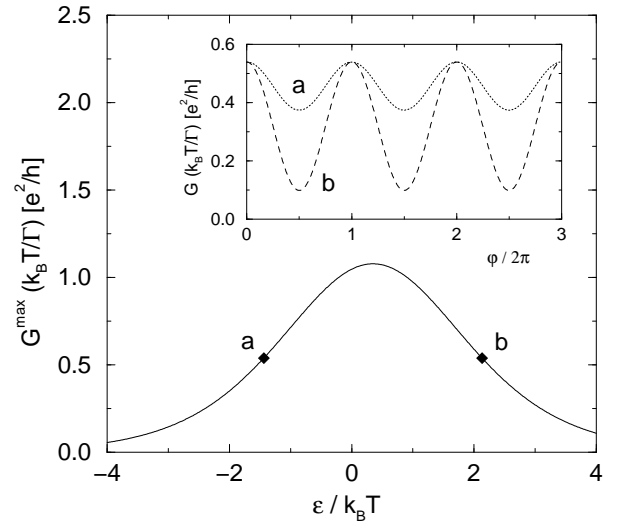


FIG. 7. Asymmetry in interference signal for AB interferometer with two QDs. Main panel: maximal conductance (i.e.,  $\varphi = 0$ ) as a function of level position. Inset: AB oscillations for the two level positions indicated by a and b in the main panel. All conductances are normalized by  $\Gamma/(k_B T)$  and plotted in units of  $e^2/h$ .

In the main panel the maximal first-order linear conductance (which occurs at  $\varphi = 0$ ) is displayed. In our simple model the resonance peak is symmetric around  $\epsilon/(k_B T) = (1/2) \ln 2$ . Now we pick two level positions

at which this maximal conductance is equal, indicated in the figure by a and b. The amplitudes of the AB oscillations at these points differ strongly from each other (inset of Fig. 7), due to the asymmetry factor  $1/[1+f(\epsilon)]^2$ . The smaller AB amplitude corresponds to the situation in which single occupation of each QD is more likely than the dots being empty.

### C. Effect of dot-dot interaction

We want to emphasize that for a proper realization of an AB interferometer which might provide full destructive interference of coherent transport channels, the two QDs should not influence each other electrostatically. Let us, e.g., consider the case of spinless electrons in an AB interferometer in which simultaneous occupation of both QDs costs the electrostatic-energy penalty  $U'$ . Again we start with Eq. (4.4), solve for the corresponding density-matrix elements (see Appendix B), and end up with

$$\left. \frac{\partial I^{\text{tot}}}{\partial V} \right|_{V=0} = 2 \left. \frac{\partial I^{\text{dot}}}{\partial V} \right|_{V=0} \times [1 - C \sin^2(\varphi/2)] \quad (4.9)$$

with

$$C = \left[ 1 + \frac{\ln^2(\beta U'/2\pi) \cos^2(\varphi/2)}{\pi^2 [1 - f(\epsilon)]^2} \right]^{-1} \quad (4.10)$$

for  $\beta\epsilon \sim 1$  and  $\beta U' \gg 1$ . At  $\varphi = 0, \pm 2\pi, \pm 4\pi, \dots$ , the total linear conductance is the sum of the conductances through the dots taken apart. For  $\varphi = \pm\pi, \pm 3\pi, \dots$ , the conductance is zero. The latter statement is not only true for first-order transport but a general fact, since it is possible to rotate the basis of the double-dot system such that one state only couples to the left reservoir and the other one to the right reservoir.<sup>17</sup>

We observe that now, since the two paths from source to drain are influencing each other electrostatically, the interference signal no longer provides a direct tool to distinguish coherent from incoherent transport through a *single* QD. The amplitude of the oscillations is reduced for increasing  $U'$  because an electron occupying one QD effectively blocks the path through the other QD, and interference is suppressed.

## V. FINITE-BIAS-INDUCED AB OSCILLATIONS

In this section we concentrate on the average number  $\langle N \rangle$  of electrons in the QD near resonance,  $|\epsilon| \lesssim k_B T$ , in the weak-coupling regime,  $\Gamma \ll k_B T$  (and  $\Gamma \ll \Delta$ ). At equilibrium,  $\langle N \rangle$  is, for both the single-dot and two-dot AB interferometer, determined by classical Boltzmann weights. The latter depend on the energy of the dot level only. In particular, they are independent of magnetic flux. (In the regime specified above, transport is dominated by first order in  $\Gamma$ , while the occupation number is

described in zeroth order.) Out of equilibrium, however, a flux dependence of  $\langle N \rangle$  might arise, as we will show in this section.

### A. Single-dot AB interferometer

In the absence of charging energy, the correction terms of the probabilities for the empty ( $\chi = 0$ ), singly-occupied ( $\chi = \sigma$  with  $\sigma = \uparrow$  or  $\downarrow$ ), and doubly-occupied dot ( $\chi = d$ ), in first order in  $t^{\text{ref}}$  are (see Appendix A)

$$P_\chi^{(1)} = \alpha_\chi \frac{2\sqrt{\Gamma_L \Gamma_R}}{\Gamma_L + \Gamma_R} |t^{\text{ref}}| \sin \varphi [f_L(\epsilon) - f_R(\epsilon)], \quad (5.1)$$

with  $\alpha_0 = 1 - F(\epsilon)$ ,  $\alpha_\sigma = F(\epsilon) - 1/2$ , and  $\alpha_d = -F(\epsilon)$ . Here we have used the definition

$$F(\epsilon) = \frac{\Gamma_L f_L(\epsilon) + \Gamma_R f_R(\epsilon)}{\Gamma_L + \Gamma_R}. \quad (5.2)$$

At finite bias voltage, the probabilities for the dot states depend on the AB flux *even in zeroth order in the intrinsic linewidth*  $\Gamma$ . Only at special values of the flux,  $\varphi = 0, \pm\pi, \pm 2\pi, \dots$ , the correction terms  $P_\chi^{(1)}$  vanish for all states  $\chi = 0, \uparrow, \downarrow, d$ , and the probabilities coincide with those of a QD without a reference arm.

The same statement is true for interacting QDs. For  $U = \infty$  we obtain correction terms of the type Eq. (5.1) with  $\alpha_0 = 1/[1 + F(\epsilon)]^2$  and  $\alpha_\sigma = -\alpha_0/2$  (see Appendix A).

For symmetric couplings,  $\Gamma_L = \Gamma_R$ , the occupation of the QD up to first order in  $t^{\text{ref}}$  is

$$\langle N \rangle = f_L(\epsilon) + f_R(\epsilon) - |t^{\text{ref}}| [f_L(\epsilon) - f_R(\epsilon)] \sin \varphi \quad (5.3)$$

for noninteracting QDs,  $U = 0$ , and

$$\langle N \rangle = \frac{f_L(\epsilon) + f_R(\epsilon)}{1 + \frac{f_L(\epsilon) + f_R(\epsilon)}{2}} - \frac{|t^{\text{ref}}| [f_L(\epsilon) - f_R(\epsilon)] \sin \varphi}{\left(1 + \frac{f_L(\epsilon) + f_R(\epsilon)}{2}\right)^2} \quad (5.4)$$

for  $U = \infty$ .

The generation of AB oscillations due to finite bias is illustrated in Fig. 8. To be specific we chose the level energy  $\epsilon$  where the conductance has its peak,  $\epsilon = 0$  for  $U = 0$  and  $\epsilon/(k_B T) = (1/2) \ln 2$ . Furthermore, we used  $|t^{\text{ref}}| = 0.1$  and chose  $\Gamma_L = \Gamma_R$  in this example.

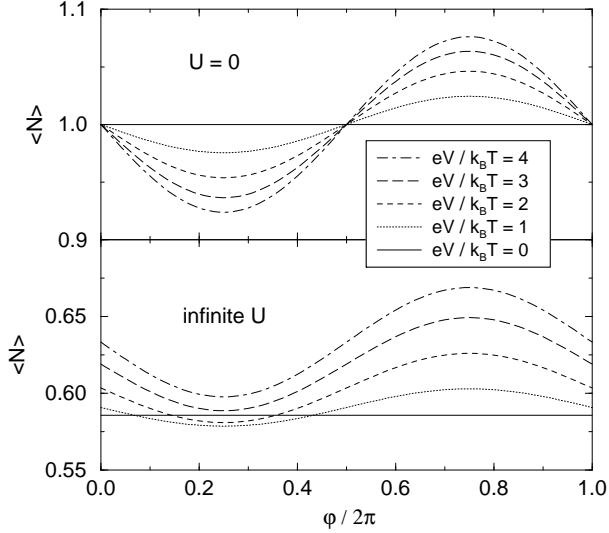


FIG. 8. Bias-voltage-induced AB oscillations of the dot occupation in a single-dot AB interferometer. The level position is tuned at the maximum of the Coulomb-oscillation peak. In equilibrium the average charge on the QD is flux independent (in lowest order in  $\Gamma$ ). With finite bias voltage, AB oscillations emerge. In this example we chose  $|t^{\text{ref}}| = 0.1$  and  $\Gamma_L = \Gamma_R$ .

### B. Two-dot AB interferometer

For the AB interferometer containing two QDs it turns out that the corrections to the diagonal matrix elements of the density matrix in lowest order in  $\Gamma$  remain zero in first order in  $V$ , i.e., in contrast to the single-dot AB interferometer, there is no bias-voltage-induced AB oscillation of the occupation of either dot in linear order in  $V$ . This changes when electrostatic inter-dot interaction is introduced (although it does not change the spatial symmetry). For the model with spinless electrons and inter-dot interaction we find that the correction for the occupation of QD 1,  $P_1^1$ , is determined (for  $\beta\epsilon \sim 1$  and  $\beta U' \gg 1$ ) by

$$\left. \frac{\partial P_1^1}{\partial V} \right|_{V=0} = -\frac{C \ln(\beta U'/2\pi)}{4\pi[1-f(\epsilon)]^2} \cdot \frac{f'(\epsilon)}{1+f(\epsilon)} \sin \varphi, \quad (5.5)$$

where the (also flux-dependent) term  $C$  is defined in Eq. (4.10). For QD 2 we get  $(\partial P_2^2/\partial V)|_{V=0} = -(\partial P_1^1/\partial V)|_{V=0}$ . All these results are derived in Appendix B.

## VI. BREAKDOWN OF PHASE LOCKING AND MORE GENERAL SYMMETRY RELATIONS

Onsager relations yield phase locking of the linear conductance through a (closed) two-terminal device, i.e., the linear conductance is symmetric under reversal of magnetic flux,  $\varphi \rightarrow -\varphi$ . Phase locking is, however, no longer

enforced in the nonlinear-response regime. In the final result for the interference current through a single-dot AB interferometer in first order in  $|t^{\text{ref}}|$ , Eq. (3.12), the first line is symmetric under  $\varphi \rightarrow -\varphi$ , but the  $\varphi$ -dependence of  $G^{(1)}$  in the second line can break this symmetry at finite bias voltages. In the following we explicitly calculate the current in lowest order in  $\Gamma$ . It will turn out that for a noninteracting QD phase locking survives even at finite bias, but is broken for interacting QDs.

In the noninteracting case we find to lowest order in  $\Gamma$  that  $\text{Im} G_\sigma^{r(1)} \sim [P_0^{(1)} + P_\uparrow^{(1)} + P_\downarrow^{(1)} + P_{\uparrow\downarrow}^{(1)}] = 0$ , which yields

$$I_R^{(1)} = \frac{4e}{h} \sqrt{\Gamma_L \Gamma_R} |t^{\text{ref}}| \cos \varphi \int' d\omega \frac{f_L(\omega) - f_R(\omega)}{\omega - \epsilon}, \quad (6.1)$$

where the prime at the integral indicates Cauchy's principal value. This proves that for a noninteracting QD phase locking is preserved even in nonequilibrium, at least in lowest order in  $\Gamma$ . It can be shown, however, that even in higher orders in  $\Gamma$  the Green's function is invariant under  $\varphi \leftrightarrow -\varphi$ , i.e., phase locking is preserved in nonequilibrium. This is due to the fact that the total current is obtained as a sum over contributions at different energies, with weights given by the nonequilibrium conditions. Each of these contributions satisfies the phase-locking symmetry separately.

This changes when interaction is turned on. For  $U = \infty$  we find that  $\text{Im} G_\sigma^{r(1)}$  is non zero, and the current reads

$$I_R^{(1)} = \frac{4e}{h} \frac{\sqrt{\Gamma_L \Gamma_R} |t^{\text{ref}}| \cos \varphi}{1+F(\epsilon)} \int' d\omega \frac{f_L(\omega) - f_R(\omega)}{\omega - \epsilon} + \frac{4\pi e (\Gamma_L \Gamma_R)^{3/2} |t^{\text{ref}}| \sin \varphi}{\Gamma^2 [1+F(\epsilon)]^2} [f_L(\epsilon) - f_R(\epsilon)]^2. \quad (6.2)$$

In addition to the first line, which corresponds to phase locking, there is a contribution proportional to  $\sin \varphi$  (second line) which breaks the symmetry under  $\varphi \leftrightarrow -\varphi$ . As we see it takes both interaction and finite bias voltage to break phase locking.

For the AB interferometer which involves two QDs, phase locking remains at finite bias, independent of whether the interaction is included or not. This is due to the symmetric setup we chose and follows from general symmetry relations, as discussed next.

### Connection between spatial symmetry and symmetry of transport coefficients

The general relation for all two-terminal setups

$$\frac{\partial I(V, \varphi)}{\partial V} = \frac{\partial I(-V, -\varphi)}{\partial V}, \quad (6.3)$$

where  $V$  is the symmetrically applied bias, yields as a direct consequence the Onsager relation

$$\left. \frac{\partial I(\varphi)}{\partial V} \right|_{V=0} = \left. \frac{\partial I(-\varphi)}{\partial V} \right|_{V=0} \quad (6.4)$$

which requires phase locking in linear response.

In addition to this symmetry Eq. (6.3), spatial symmetries can be exploited as well. Let us first consider an AB interferometer with a single QD. If  $\Gamma_L = \Gamma_R$  then the system remains invariant if it is mirrored with respect to a vertical axis and the chemical potentials of the left and right leads are exchanged. This leads only to Eq. (6.3) and does not induce a new relation.

The situation is more complex for the AB interferometer made out of two QDs. We assume that the QDs are identical. The coupling of the QDs to the leads, however, may be different. We consider three different cases in which the system has a spatial symmetry, see Fig. 9.

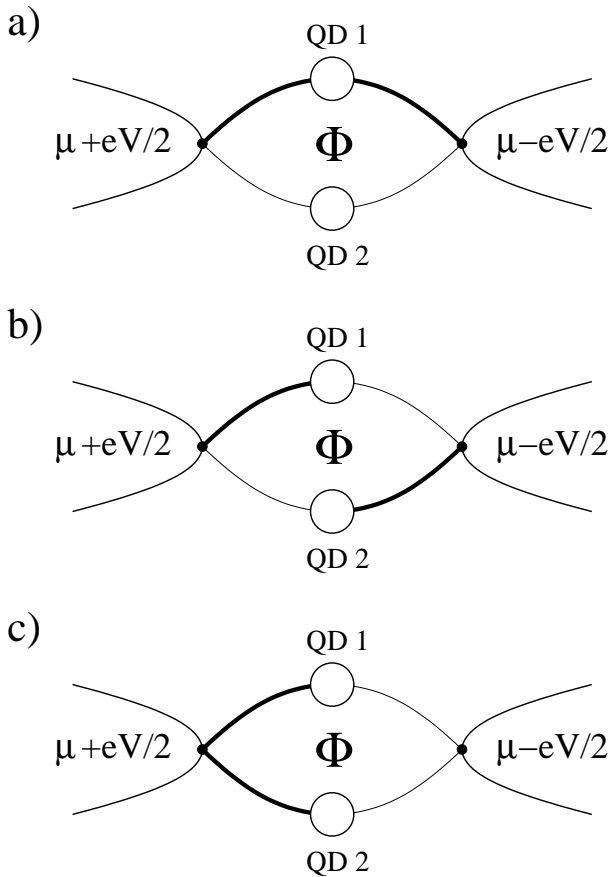


FIG. 9. Two-dot AB interferometers with different spatial symmetry. Thick and thin lines indicate stronger and weaker tunnel coupling, respectively. a) possesses mirror symmetry with respect to a vertical axis, b) is invariant under rotation at angle  $\pi$ , and c) has mirror symmetry with respect to a horizontal axis. In cases b) and c) phase locking is preserved even for finite bias.

If  $|t_{L,\text{dot}1}| = |t_{R,\text{dot}1}|$  and  $|t_{L,\text{dot}2}| = |t_{R,\text{dot}2}|$  (see Fig. 9a) the system has mirror symmetry with respect to a vertical axis only, and the resulting symmetry relation

$$\frac{\partial I(V, \varphi)}{\partial V} = \frac{\partial I(-V, -\varphi)}{\partial V} \quad (6.5)$$

coincides with Eq (6.3).

If  $|t_{L,\text{dot}1}| = |t_{R,\text{dot}2}|$  and  $|t_{R,\text{dot}1}| = |t_{L,\text{dot}2}|$  (see Fig. 9b) the system is invariant under rotation at angle  $\pi$  in the plane and reversal of  $V$ . As a consequence

$$\frac{\partial I(V, \varphi)}{\partial V} = \frac{\partial I(-V, \varphi)}{\partial V}. \quad (6.6)$$

If  $|t_{L,\text{dot}1}| = |t_{L,\text{dot}2}|$  and  $|t_{R,\text{dot}1}| = |t_{R,\text{dot}2}|$  (see Fig. 9c) the system has mirror symmetry with respect to a horizontal axis. This implies

$$\frac{\partial I(V, \varphi)}{\partial V} = \frac{\partial I(V, -\varphi)}{\partial V}. \quad (6.7)$$

In the two latter cases phase locking occurs, which either follows directly or after making use of Eq. (6.3). This is a consequence of spatial symmetry. In the first case, or without any spatial symmetry, breaking of phase locking may be possible for finite voltages.

## VII. SUMMARY AND DISCUSSION

The focus of this work is the interplay between coherent and incoherent transport channels of a mesoscopic setup. We specifically address the issue of transport through a quantum dot. To stress the difference between dephasing processes (which do not require any energy exchange) and inelastic scattering (which, of course, may also introduce incoherent transport), we have chosen to discuss spin-flip processes as the source of dephasing. Our analysis then elucidates some important facets of electronic spin transport. Central to our analysis is the fact that the existence of decohering spin-flip channels requires the presence of electron-electron interaction (in our model the constant capacitance term). We have shown explicitly that in the absence of such interaction the contributions from the spin-flip channels cancel out.

In order to quantify and study the “degree of coherence” in the system we had to resort to interferometry setups. This is why we have embedded our system in an Aharonov-Bohm circuit, in line with recent experiments. As we present results for the AB amplitude of the transmitted current (as compared with the flux-insensitive component of the current), our results are closely related the “visibility”, employed by some experimentalists in this context.

Technically we have performed a systematic analysis of first- and second-order (in the QD-lead coupling,  $\Gamma$ ) transport through AB interferometers containing either one or two QDs. As a consequence, in the Coulomb blockade valley with one dot level being singly-occupied only one half of the low-temperature (yet  $T > T_K$ ) transport is coherent. This is to be contrasted with the case of all dot levels being either empty or doubly occupied,

where transport is fully coherent. The conclusions of our analysis, performed for a QD with a single level, are generalized to a multilevel QD. In contrast to expectations based on a sequential-tunneling picture, we have proved that even in first-order transport, the transmission is at least partially coherent. Our formalism allows to cover the nonlinear-response regime, too. We predict bias-voltage-induced AB oscillations in the occupation number of the QD of a single-dot AB interferometer.

An important outcome of our analysis is the partial suppression of the AB conductance oscillations which, in the presence of e-e interactions, is asymmetric with respect to the position of the Coulomb peaks. This asymmetry is a manifestation of the presence of incoherent transport channels, whose number is different between the two sides of a Coulomb peak. Our asymmetry effect (calculated in low orders in  $\Gamma$ ) increases with lowering the temperature. The physical picture is expected to change, though, as the temperature is lowered towards and beyond the Kondo temperature  $T_K$ . In this case, the local spin of the QD is screened by the lead electron spins. At zero temperature the QD is seen by the transmitted electrons as a pure static potential scatterer, i.e., no spin-flip appears. We therefore expect an increase of the coherent transport contribution when the temperature is decreased below  $T_K$ , and a gradual disappearance of our asymmetry effect. This shows that while our coherence asymmetry effect may provide information comparable to that obtained through the Kondo physics (i.e., the QD's spin), the latter reflects different physics. We also note that the asymmetry we refer to concerns the magnitude of the AB amplitudes at two points on different sides of the Coulomb blockade peak, which correspond to the same total (flux-averaged) conductance. Our asymmetry *does not imply an asymmetric line shape* of the conductance, and therefore is different from the Fano mechanism. The presence of such asymmetries in the experiment will be discussed elsewhere.<sup>48</sup> The results of our analysis suggest that one may use this asymmetry to probe the total spin of a QD; we discuss how this asymmetry is suppressed for multilevel QDs, as the level spacing is reduced.

We have included in our analysis a brief discussion of time-reversal symmetry in the problem, specifically the issue of phase locking. The latter is usually presented as an outcome of Onsager relations. We have shown how, in general, it breaks down at finite bias voltages. In certain cases, however, we find that phase locking is preserved due to spatial symmetry of the setup.

## ACKNOWLEDGEMENT

We acknowledge helpful discussions with B. Altshuler, N. Andrei, D. Boese, P. Coleman, A. de Silva, L. Glazman, Y. Imry, B. Kubala, Y. Nazarov, Y. Oreg, H. Schoeller, and G. Schön. J.K. acknowledges the Ein-

stein Center for partially supporting his visits to the Weizmann Institute of Science. This work was supported by the Deutsche Forschungsgemeinschaft under the Emmy-Noether program, the U.S.-Israel Binational Science Foundation, the Minerva Foundation, the Israel Science Foundation of the Israel Academy of Sciences and Humanities Centers of Excellence Program and by the Deutsch-Israelisches Projekt.

## APPENDIX A: DENSITY MATRIX FOR SINGLE-DOT AB INTERFEROMETER

In this appendix we present the somewhat technical part of calculating the density-matrix elements for the single-dot AB interferometer. The derivation is based on the real-time transport theory developed in Refs. 29,34. The starting point is the generalized stationary master equation in Liouville space,

$$(\epsilon_{\chi_1} - \epsilon_{\chi_2}) P_{\chi_2}^{\chi_1} + \sum_{\chi'_1, \chi'_2} P_{\chi_2}^{\chi'_1} \Sigma_{\chi'_2, \chi_2}^{\chi'_1, \chi_1} = 0, \quad (\text{A1})$$

where  $\chi_1$  and  $\chi_2$  denote any state for the QD,  $\epsilon_{\chi_1}$  and  $\epsilon_{\chi_2}$  are the corresponding energies, and  $P_{\chi_2}^{\chi_1} = \langle |\chi_2\rangle \langle \chi_1| \rangle$  is a matrix element of the reduced density matrix for the QD subsystem. The diagonal matrix elements  $P_{\chi_1} \equiv P_{\chi_1}^{\chi_1}$  are nothing but the probabilities to find the system in a given state  $\chi_1$ .

The matrix elements  $P$  of the density matrix are connected to each other in Eq. (A1) by the terms  $\Sigma_{\chi'_2, \chi_2}^{\chi'_1, \chi_1}$  which can be viewed as generalized transition rates in Liouville space. They are defined as the irreducible self-energy parts of the propagation in Liouville space and are represented as diagram blocks on a Keldysh contour. For a detailed derivation of this diagrammatic language, the generalized master equation, and the rules on how to calculate the value of a diagram we refer to Refs. 29,34.

In the present context we calculate the corrections linear in  $t^{\text{ref}}$  to the probabilities for the dot states. We concentrate on the regime where the dot level is tuned close to resonance, i.e., we determine the probabilities in zeroth order in  $\Gamma$ . To this end we need the self-energy parts  $\Sigma$  to lowest (first) order in  $\Gamma$ . The possible dot states  $\chi$  are labeled by 0 for an empty QD,  $\sigma$  for single occupancy with spin  $\sigma = \uparrow, \downarrow$ , and  $d$  for double occupancy.

First, we observe that in the generalized master equation Eq. (A1) the probabilities  $P_\chi = P_\chi^\chi$  couple to diagonal matrix elements only. This has to do with the fact that the  $z$  component of the spin is a conserved quantity. As a consequence, only self-energy parts of the type  $\Sigma_{\chi, \chi'} \equiv \Sigma_{\chi, \chi'}^{\chi, \chi'}$  enter. We get to zeroth order (indicated by the superscript (0)) in  $t^{\text{ref}}$  the master equations

$$P_0^{(0)} \Sigma_{00}^{(0)} + 2P_\sigma^{(0)} \Sigma_{\sigma 0}^{(0)} + P_d^{(0)} \Sigma_{d0}^{(0)} = 0 \quad (\text{A2})$$

$$P_0^{(0)} \Sigma_{0d}^{(0)} + 2P_\sigma^{(0)} \Sigma_{\sigma d}^{(0)} + P_d^{(0)} \Sigma_{dd}^{(0)} = 0 \quad (\text{A3})$$



together with the normalization condition  $P_0^{(0)} + 2P_\sigma^{(0)} + P_d^{(0)} = 1$ . The diagrammatic representation of the irreducible self-energy parts are shown in Fig. 10.

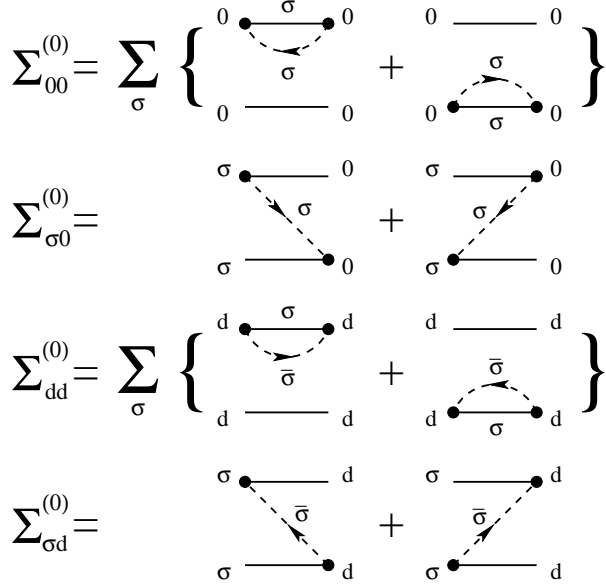


FIG. 10. Irreducible self-energy parts to zeroth order in  $t^{\text{ref}}$  (and first order in  $\Gamma$ ).

There are two horizontal lines representing the forward (upper line) and backward (lower line) propagators on the Keldysh contour. Vertices (full dots) indicate tunneling from the QD to the lead or vice versa. They are connected in pairs by tunnel lines (dashed lines) representing contractions of lead electron operators. Depending on the order of the annihilation and creation operators, specified by the arrows, the tunnel lines contribute with a Fermi function  $f_r$  (if the line goes backward with respect to the Keldysh contour) or  $1 - f_r$  (if the line goes forward),  $r = L/R$ , times  $|t_r|^2 N_r = \Gamma_r/(2\pi)$ , where  $N_r$  is the density of states in reservoir  $r$ . Along the tunnel lines and the forward and backward propagators we assign the proper dot states such that the particle number and  $z$  component of the spin are conserved at each vertex.

It is easy to see that it is impossible to construct a diagram for  $\Sigma_{d0}$  or  $\Sigma_{0d}$  to first order in  $\Gamma$ , i.e.,  $\Sigma_{d0} = \Sigma_{0d} = 0$ . The other diagrams are depicted in Fig. 10. As an example we calculate  $\Sigma_{\sigma 0}^{(0)}$  explicitly, using the diagrammatic rules derived in Refs. 29,34. The tunnel line contributes with  $\Gamma_r/(2\pi)[1 - f_r(\omega)]$ . There is a minus sign for each vertex on the backward propagator. This yields a total minus sign for the diagram under consideration. For each segment between two vertices there is a resolvent  $1/(\Delta E + i0^+)$ , where  $\Delta E$  is the difference between the energy on the left-going lines and right-going lines (including the propagators and the tunnel lines). For the left diagram we obtain  $1/(\epsilon - \omega + i0^+)$ . Finally, we integrate over the energy  $\omega$  of the tunnel line and sum over the reservoir index  $r$  to get

$$- \sum_r \frac{\Gamma_r}{2\pi} \int d\omega \frac{1 - f_r(\omega)}{\epsilon - \omega + i0^+}. \quad (\text{A4})$$

The value of the right diagram is the same except for the denominator which now reads  $\omega - \epsilon + i0^+$ . After making use of  $1/(x + i0^+) = P(1/x) - i\pi\delta(x)$  we can evaluate the integrals. The final result (for all diagrams shown in Fig. 10) is

$$\Sigma_{00}^{(0)} = -2i\Gamma F(\epsilon) \quad (\text{A5})$$

$$\Sigma_{\sigma 0}^{(0)} = i\Gamma[1 - F(\epsilon)] \quad (\text{A6})$$

$$\Sigma_{dd}^{(0)} = -2i\Gamma[1 - F(\epsilon + U)] \quad (\text{A7})$$

$$\Sigma_{\sigma d}^{(0)} = i\Gamma F(\epsilon + U), \quad (\text{A8})$$

where we have used the definitions  $F(\omega) = [\Gamma_L f_L(\omega) + \Gamma_R f_R(\omega)]/(\Gamma_L + \Gamma_R)$  and  $\Gamma = \Gamma_L + \Gamma_R$ . This yields the solution

$$P_0^{(0)} = \frac{[1 - F(\epsilon)][1 - F(\epsilon + U)]}{F(\epsilon) + 1 - F(\epsilon + U)} \quad (\text{A9})$$

$$P_\sigma^{(0)} = \frac{F(\epsilon)[1 - F(\epsilon + U)]}{F(\epsilon) + 1 - F(\epsilon + U)} \quad (\text{A10})$$

$$P_d^{(0)} = \frac{F(\epsilon)F(\epsilon + U)}{F(\epsilon) + 1 - F(\epsilon + U)}. \quad (\text{A11})$$

In equilibrium  $F(\omega) = f(\omega)$ , and we recover the classical Boltzmann factors which determine the probabilities,  $P_0^{(0)} = 1/Z$ ,  $P_\sigma^{(0)} = \exp(-\beta\epsilon)/Z$ , and  $P_d^{(0)} = \exp[-\beta(2\epsilon + U)]/Z$  with  $Z = 1 + 2\exp(-\beta\epsilon) + \exp[-\beta(2\epsilon + U)]$ .

The effect of the reference arm on the QD shows up in the correction terms to the probabilities in first order in  $t^{\text{ref}}$ . The master equations to solve are

$$P_0^{(0)}\Sigma_{00}^{(1)} + 2P_\sigma^{(0)}\Sigma_{\sigma 0}^{(1)} + P_0^{(1)}\Sigma_{00}^{(0)} + 2P_\sigma^{(1)}\Sigma_{\sigma 0}^{(0)} = 0 \quad (\text{A12})$$

$$P_d^{(0)}\Sigma_{dd}^{(1)} + 2P_\sigma^{(0)}\Sigma_{\sigma d}^{(1)} + P_d^{(1)}\Sigma_{dd}^{(0)} + 2P_\sigma^{(1)}\Sigma_{\sigma d}^{(0)} = 0 \quad (\text{A13})$$

along with the normalization condition  $P_0^{(1)} + 2P_\sigma^{(1)} + P_d^{(1)} = 0$ . The diagrams for the self-energy part to first order in  $t^{\text{ref}}$  are shown in Fig. 11.

$$\begin{aligned}
\Sigma_{00}^{(1)} &= \sum_{\sigma} \left\{ \begin{array}{l}
\begin{array}{c} 0 \quad 0 \\ \text{L} \quad \text{R} \\ \hline \sigma \quad 0 \\ \text{0} \end{array} + \begin{array}{c} 0 \quad 0 \\ \text{R} \\ \hline \text{0} \quad \text{L} \\ \sigma \quad 0 \end{array} + \begin{array}{c} 0 \quad 0 \\ \text{L} \quad \text{R} \\ \hline \sigma \quad 0 \\ \text{0} \end{array} + \begin{array}{c} 0 \quad 0 \\ \text{L} \quad \text{R} \\ \hline \sigma \quad \sigma \\ \text{0} \end{array} + \begin{array}{c} 0 \quad 0 \\ \text{L} \quad \text{R} \\ \hline \sigma \quad \text{0} \\ \text{0} \end{array} + \begin{array}{c} 0 \quad 0 \\ \text{L} \quad \text{R} \\ \hline \sigma \quad \text{0} \\ \text{0} \end{array} \\
+ \begin{array}{c} 0 \quad 0 \\ \text{R} \quad \text{L} \\ \hline \sigma \quad 0 \\ \text{0} \end{array} + \begin{array}{c} 0 \quad 0 \\ \text{R} \quad \text{L} \\ \hline \text{0} \quad \sigma \\ \sigma \quad 0 \end{array} + \begin{array}{c} 0 \quad 0 \\ \text{R} \quad \text{L} \\ \hline \sigma \quad 0 \\ \text{0} \end{array} + \begin{array}{c} 0 \quad 0 \\ \text{R} \quad \text{L} \\ \hline \sigma \quad \sigma \\ \text{0} \end{array} + \begin{array}{c} 0 \quad 0 \\ \text{R} \quad \text{L} \\ \hline \sigma \quad \text{0} \\ \text{0} \end{array} + \begin{array}{c} 0 \quad 0 \\ \text{R} \quad \text{L} \\ \hline \sigma \quad \text{0} \\ \text{0} \end{array} \\
+ (L \leftrightarrow R) \end{array} \right\} \\
\Sigma_{\sigma 0}^{(1)} &= \left\{ \begin{array}{l}
\begin{array}{c} \sigma \quad 0 \\ \text{L} \quad \text{R} \\ \hline \sigma \quad 0 \\ \text{0} \end{array} + \begin{array}{c} \sigma \quad 0 \\ \text{L} \quad \text{R} \\ \hline \sigma \quad \sigma \\ \text{0} \end{array} + \begin{array}{c} \sigma \quad 0 \\ \text{L} \quad \text{R} \\ \hline \sigma \quad 0 \\ \text{0} \end{array} + \begin{array}{c} \sigma \quad 0 \\ \text{L} \quad \text{R} \\ \hline \sigma \quad \sigma \\ \text{0} \end{array} + \begin{array}{c} \sigma \quad 0 \\ \text{L} \quad \text{R} \\ \hline \sigma \quad \text{0} \\ \text{0} \end{array} + \begin{array}{c} \sigma \quad 0 \\ \text{L} \quad \text{R} \\ \hline \sigma \quad \text{0} \\ \text{0} \end{array} \\
+ \begin{array}{c} \sigma \quad 0 \\ \text{R} \quad \text{L} \\ \hline \sigma \quad 0 \\ \text{0} \end{array} + \begin{array}{c} \sigma \quad 0 \\ \text{R} \quad \text{L} \\ \hline \sigma \quad \sigma \\ \text{0} \end{array} + \begin{array}{c} \sigma \quad 0 \\ \text{R} \quad \text{L} \\ \hline \sigma \quad 0 \\ \text{0} \end{array} + \begin{array}{c} \sigma \quad 0 \\ \text{R} \quad \text{L} \\ \hline \sigma \quad \sigma \\ \text{0} \end{array} + \begin{array}{c} \sigma \quad 0 \\ \text{R} \quad \text{L} \\ \hline \sigma \quad \text{0} \\ \text{0} \end{array} + \begin{array}{c} \sigma \quad 0 \\ \text{R} \quad \text{L} \\ \hline \sigma \quad \text{0} \\ \text{0} \end{array} \\
+ (L \leftrightarrow R) \end{array} \right\} \\
\Sigma_{d d}^{(1)} &= \sum_{\sigma} \left\{ \begin{array}{l}
\begin{array}{c} d \quad d \\ \text{L} \quad \text{R} \\ \hline \sigma \quad d \\ \text{d} \end{array} + \begin{array}{c} d \quad d \\ \text{L} \quad \text{R} \\ \hline \text{d} \quad \sigma \\ \sigma \quad d \end{array} + \begin{array}{c} d \quad d \\ \text{L} \quad \text{R} \\ \hline \sigma \quad d \\ \text{d} \end{array} + \begin{array}{c} d \quad d \\ \text{L} \quad \text{R} \\ \hline \sigma \quad \sigma \\ \text{d} \end{array} + \begin{array}{c} d \quad d \\ \text{L} \quad \text{R} \\ \hline \sigma \quad \text{d} \\ \text{d} \end{array} + \begin{array}{c} d \quad d \\ \text{L} \quad \text{R} \\ \hline \sigma \quad \text{d} \\ \text{d} \end{array} \\
+ \begin{array}{c} d \quad d \\ \text{R} \quad \text{L} \\ \hline \sigma \quad d \\ \text{d} \end{array} + \begin{array}{c} d \quad d \\ \text{R} \quad \text{L} \\ \hline \text{d} \quad \sigma \\ \sigma \quad d \end{array} + \begin{array}{c} d \quad d \\ \text{R} \quad \text{L} \\ \hline \sigma \quad d \\ \text{d} \end{array} + \begin{array}{c} d \quad d \\ \text{R} \quad \text{L} \\ \hline \sigma \quad \sigma \\ \text{d} \end{array} + \begin{array}{c} d \quad d \\ \text{R} \quad \text{L} \\ \hline \sigma \quad \text{d} \\ \text{d} \end{array} + \begin{array}{c} d \quad d \\ \text{R} \quad \text{L} \\ \hline \sigma \quad \text{d} \\ \text{d} \end{array} \\
+ (L \leftrightarrow R) \end{array} \right\} \\
\Sigma_{\sigma d}^{(1)} &= \left\{ \begin{array}{l}
\begin{array}{c} \sigma \quad d \\ \text{L} \quad \text{R} \\ \hline \sigma \quad d \\ \text{d} \end{array} + \begin{array}{c} \sigma \quad d \\ \text{L} \quad \text{R} \\ \hline \sigma \quad \sigma \\ \text{d} \end{array} + \begin{array}{c} \sigma \quad d \\ \text{L} \quad \text{R} \\ \hline \sigma \quad d \\ \text{d} \end{array} + \begin{array}{c} \sigma \quad d \\ \text{L} \quad \text{R} \\ \hline \sigma \quad \sigma \\ \text{d} \end{array} + \begin{array}{c} \sigma \quad d \\ \text{L} \quad \text{R} \\ \hline \sigma \quad \text{d} \\ \text{d} \end{array} + \begin{array}{c} \sigma \quad d \\ \text{L} \quad \text{R} \\ \hline \sigma \quad \text{d} \\ \text{d} \end{array} \\
+ \begin{array}{c} \sigma \quad d \\ \text{R} \quad \text{L} \\ \hline \sigma \quad d \\ \text{d} \end{array} + \begin{array}{c} \sigma \quad d \\ \text{R} \quad \text{L} \\ \hline \sigma \quad \sigma \\ \text{d} \end{array} + \begin{array}{c} \sigma \quad d \\ \text{R} \quad \text{L} \\ \hline \sigma \quad d \\ \text{d} \end{array} + \begin{array}{c} \sigma \quad d \\ \text{R} \quad \text{L} \\ \hline \sigma \quad \sigma \\ \text{d} \end{array} + \begin{array}{c} \sigma \quad d \\ \text{R} \quad \text{L} \\ \hline \sigma \quad \text{d} \\ \text{d} \end{array} + \begin{array}{c} \sigma \quad d \\ \text{R} \quad \text{L} \\ \hline \sigma \quad \text{d} \\ \text{d} \end{array} \\
+ (L \leftrightarrow R) \end{array} \right\}
\end{aligned}$$

FIG. 11. Irreducible self-energy parts to first order in  $t^{\text{ref}}$  (and first order in  $\Gamma$ ). There are two kinds of vertices: single vertices (full dots), which represent tunneling between QD and leads, and double vertices (open dots), which indicate direct tunneling between the leads. We show explicitly all diagrams with direct tunneling from left to right (they are proportional to  $e^{i\varphi}$ ). The remaining diagrams are obtained by exchanging the labels  $L$  and  $R$  for the left and right lead everywhere (those are proportional to  $e^{-i\varphi}$ ).

Here, another type of vertex has to be introduced which represents direct tunneling from one lead to the other. Such a vertex is connected to two tunnel lines (“double vertex”) since it represents two lead electron operators which are contracted with another operator of the same lead each. As a consequence we encounter objects made of two tunnel lines connecting one double vertex with two single vertices. Each line contributes with  $f_r$  or  $1 - f_r$ , and the total multiplication factor is  $N_L N_R t_L t_R |\tilde{t}| = |t^{\text{ref}}| \sqrt{\Gamma_L \Gamma_R} / (4\pi^2)$  times  $e^{\pm i\varphi}$ . The upper (lower) sign applies if the incoming line into the double vertex belongs to the left (right) lead.

Again we evaluate one diagram explicitly, namely the first one contributing to  $\Sigma_{\sigma 0}^{(1)}$  as shown in Fig. 11. We find

$$\int d\omega_L \int d\omega_R \frac{f_L(\omega_L)[1 - f_R(\omega_R)]}{(\omega_L - \omega_R + i0^+)(\epsilon - \omega_R + i0^+)} \quad (\text{A14})$$

times  $|t^{\text{ref}}| e^{i\varphi} \sqrt{\Gamma_L \Gamma_R} / (4\pi^2)$ . There is one minus sign due to the vertex on the lower propagator. This is, however, canceled by another minus sign coming from the ordering of the Fermi operators: in the diagrammatic language, each crossing of tunnel lines introduces a minus sign (to apply this rule view the double vertex as two separate vertices lying close together, where the vertex connected to the incoming line comes first with respect to the Keldysh contour).<sup>49</sup>

We note that for all self-energy parts shown in Fig. 11 the fifth and sixth diagrams cancel each other out since they differ by a minus sign due to the vertices on the lower propagator. The same holds for the eleventh and twelfth diagrams.

After collecting all contributions we end up with

$$\Sigma_{\sigma 0}^{(1)} = i \sin \varphi \sqrt{\Gamma_L \Gamma_R} |t^{\text{ref}}| [f_L(\epsilon) - f_R(\epsilon)] \quad (\text{A15})$$

$$\Sigma_{\sigma d}^{(1)} = -i \sin \varphi \sqrt{\Gamma_L \Gamma_R} |t^{\text{ref}}| [f_L(\epsilon + U) - f_R(\epsilon + U)] \quad (\text{A16})$$

as well as  $\Sigma_{00}^{(1)} = 2\Sigma_{\sigma 0}^{(1)}$  and  $\Sigma_{dd}^{(1)} = 2\Sigma_{\sigma d}^{(1)}$ .

The results for  $P_\chi^{(1)}$  are lengthy expressions. They simplify, however, for either  $U = 0$  or  $U = \infty$ . For these limits they are given by Eq. (5.1).

## APPENDIX B: DENSITY MATRIX FOR TWO-DOT AB INTERFEROMETER

In this appendix we determine the off-diagonal matrix element  $P_{2\sigma}^{1\sigma}$  in zeroth order in  $\Gamma$  for the two-dot AB interferometer. These results are needed for the evaluation of Eq. (4.4). To achieve this goal we expand Eq. (A1) up to zeroth and first order in  $\Gamma$ . The irreducible self-energy parts  $\Sigma$  have contributions of order  $\Gamma$  and higher. As a consequence, the zeroth order expansion of Eq. (A1) yields that all off-diagonal matrix elements  $P_{\chi_2}^{\chi_1}$  with  $\chi_1 \neq \chi_2$  can only arise for  $\epsilon_{\chi_1} = \epsilon_{\chi_2}$ . Otherwise,  $P_{\chi_2}^{\chi_1}$  vanishes.

The calculation in this section is based on the same diagrammatic language as introduced in the previous appendix. In the two-dot AB interferometer there is no direct tunneling between leads, i.e., no double vertices will appear in the diagrams. Since constructing and evaluating the diagrams is straightforward along the line indicated for the single-dot AB interferometer in the previous appendix, we refrain from drawing them explicitly.

### 1. No interaction

In the case of noninteracting QDs,  $U = 0$ , the two channels provided by the spin degree of freedom do not influence each other. The Hamiltonian is just the sum of two identical models, one for each spin. In this case it is sufficient to consider a simpler model with spinless electrons and multiply the final expressions for the current by a trivial factor of 2. This simplifies both the calculations and the notations.

The Hilbert space of the double-dot system is, then, four dimensional: the double dot can be empty ( $\chi = 0$ ), singly occupied with the electron in dot 1 or 2 ( $\chi = 1, 2$ ), or both dots are filled ( $\chi = 12$ ). The corresponding energies are 0,  $\epsilon$ , and  $2\epsilon$ , respectively. The density matrix has 16 matrix elements. Four of them are the diagonal matrix elements  $P_0^0$ ,  $P_1^1$ ,  $P_2^2$ , and  $P_{12}^{12}$ . They are all real and positive. Since the transformation  $1 \leftrightarrow 2$  and  $V \leftrightarrow -V$  does not change the system, the three combinations  $P_0^0$ ,  $P_1^1 + P_2^2$ , and  $P_{12}^{12}$  are even in  $V$ , while the combination  $P_1^1 - P_2^2$  is odd. There are two nonvanishing off-diagonal matrix elements,  $P_1^2$  and  $P_2^1$ . All others are zero in zeroth order of  $\Gamma$  since the energies of the corresponding states differ from each other. The hermiticity of the density matrix implies  $P_1^2 = (P_2^1)^*$ .

In equilibrium,  $V = 0$ , the diagonal matrix elements  $P_\chi^X$  are probabilities for the state  $\chi$  determined by classical Boltzmann factors  $\exp(-\beta\epsilon_\chi)$ , and all off-diagonal matrix elements vanish. Our goal is to determine the linear corrections in  $V$ . Only the elements which are odd in  $V$  have a finite correction. These elements are  $P_1^1 - P_2^2$  and  $\text{Im} P_2^1$ .

In the following, we write  $P = \bar{P} + \hat{P} + \dots$  and  $\Sigma = \bar{\Sigma} + \hat{\Sigma} + \dots$  for the zeroth and first order in  $V$ . It turns out that there are two independent equations which relate the first-order corrections  $\hat{P}_1^1 = -\hat{P}_2^2$  and  $\text{Im} \hat{P}_2^1 = -\text{Im} \hat{P}_1^2$  to the zeroth-order terms  $\bar{P}_0^0$ ,  $\bar{P}_1^1 = \bar{P}_2^2$ , and  $\bar{P}_{12}^{12}$ .

We will make use of the relations  $\bar{P}_\chi^{X'} = \bar{P}_{\tilde{\chi}}^{\tilde{X}'}$  and  $\bar{\Sigma}_{\chi, \chi'}^{X, X''} = \bar{\Sigma}_{\tilde{\chi}, \tilde{\chi}'}^{\tilde{X}, \tilde{X}''}$  in equilibrium and  $\hat{P}_\chi^{X'} = -\hat{P}_{\tilde{\chi}}^{\tilde{X}'}$  and  $\hat{\Sigma}_{\chi, \chi'}^{X, X''} = -\hat{\Sigma}_{\tilde{\chi}, \tilde{\chi}'}^{\tilde{X}, \tilde{X}''}$  for the first-order correction in  $V$ , where  $\tilde{\chi}$  is obtained from  $\chi$  by the transformation  $1 \leftrightarrow 2$ . For transition from diagonal states in Liouville space to diagonal ones we find  $\hat{\Sigma}_{\chi, \chi'}^{X, X'} = 0$ . Finally, we drop all  $\Sigma$  terms which connect states in Liouville space that are not compatible, at least to lowest order in  $\Gamma$ . As a consequence the master equations for the linear correction in

$V$  read

$$0 = \hat{P}_1^1 \bar{\Sigma}_{1,1}^{1,1} + \hat{P}_2^1 \left( \bar{\Sigma}_{2,1}^{1,1} - \bar{\Sigma}_{1,1}^{2,1} \right) \quad (\text{B1})$$

$$0 = \hat{P}_2^1 \bar{\Sigma}_{2,2}^{1,1} + \hat{P}_1^1 \left( \bar{\Sigma}_{1,2}^{1,1} - \bar{\Sigma}_{2,2}^{2,1} \right) + \bar{P}_0^0 \hat{\Sigma}_{0,2}^{0,1} + \bar{P}_1^1 \left( \hat{\Sigma}_{1,2}^{1,1} + \hat{\Sigma}_{2,2}^{2,1} \right) + \bar{P}_{12}^{12} \hat{\Sigma}_{12,2}^{12,1}. \quad (\text{B2})$$

We calculate all diagrams explicitly and find

$$\bar{\Sigma}_{1,1}^{1,1} = \bar{\Sigma}_{2,2}^{1,1} = -i\Gamma \quad (\text{B3})$$

$$\bar{\Sigma}_{2,1}^{1,1} - \bar{\Sigma}_{1,1}^{2,1} = \bar{\Sigma}_{1,2}^{1,1} - \bar{\Sigma}_{2,2}^{2,1} = 0 \quad (\text{B4})$$

for  $V = 0$ , and

$$\hat{\Sigma}_{0,2}^{0,1} = \frac{\hat{\Sigma}_{1,2}^{1,1} + \hat{\Sigma}_{2,2}^{2,1}}{2} = \hat{\Sigma}_{12,2}^{12,1} = \frac{\Gamma}{2} eV f'(\epsilon) \sin \frac{\varphi}{2} \quad (\text{B5})$$

for the first-order correction in  $V$ . This leads to

$$\hat{P}_1^1 = 0 \quad (\text{B6})$$

$$\hat{P}_2^1 = -\frac{i}{2} eV f'(\epsilon) \sin \frac{\varphi}{2}. \quad (\text{B7})$$

## 2. Infinite charging energy

It is straightforward to generalize the previous discussion to the case of QDs with infinite charging energy,  $U = \infty$ . In addition to the label for dots 1 and 2, we use  $\sigma$  to label the spin, and  $\bar{\sigma}$  for the spin opposite to  $\sigma$ . Since infinite charging energy suppresses all states where either one or both dots are occupied with two electrons, the Hilbert space has nine dimensions. Spin symmetry reduces the number of independent diagonal matrix elements from nine to five,  $P_0^0$ ,  $P_{1\sigma}^{1\sigma} = P_{1\bar{\sigma}}^{1\bar{\sigma}}$ ,  $P_{2\sigma}^{2\sigma} = P_{2\bar{\sigma}}^{2\bar{\sigma}}$ ,  $P_{1\sigma 2\sigma}^{1\sigma 2\sigma} = P_{1\bar{\sigma} 2\bar{\sigma}}^{1\bar{\sigma} 2\bar{\sigma}}$ , and  $P_{1\sigma 2\bar{\sigma}}^{1\sigma 2\bar{\sigma}} = P_{1\bar{\sigma} 2\sigma}^{1\bar{\sigma} 2\sigma}$ . They are all real. Since the transformation  $1 \leftrightarrow 2$  and  $V \leftrightarrow -V$  does not change the system, the four combinations  $P_0^0$ ,  $P_{1\sigma}^{1\sigma} + P_{2\sigma}^{2\sigma}$ ,  $P_{1\sigma 2\sigma}^{1\sigma 2\sigma}$ , and  $P_{1\sigma 2\bar{\sigma}}^{1\sigma 2\bar{\sigma}}$  are even in  $V$ , while the combination  $P_{1\sigma}^{1\sigma} - P_{2\sigma}^{2\sigma}$  is odd.

We are only interested in those off-diagonal matrix elements for which the projection on the  $z$  direction of the total spin of the corresponding states is the same. There are six of them, but again spin symmetry reduced the number of independent elements to three,  $P_{2\sigma}^{1\sigma} = P_{2\bar{\sigma}}^{1\bar{\sigma}}$ ,  $P_{1\sigma}^{2\sigma} = P_{1\bar{\sigma}}^{2\bar{\sigma}}$ , and  $P_{1\sigma 2\sigma}^{1\bar{\sigma} 2\sigma} = P_{1\bar{\sigma} 2\sigma}^{1\sigma 2\bar{\sigma}}$ . Furthermore,  $P_{1\sigma}^{2\sigma} = (P_{2\sigma}^{1\sigma})^*$ . There are only two independent variables,  $P_{1\sigma}^{1\sigma} - P_{2\sigma}^{2\sigma}$  and  $\text{Im} P_{2\sigma}^{1\sigma}$ , which have a linear correction in  $V$ .

Again we write  $P = \bar{P} + \hat{P} + \dots$  and  $\Sigma = \bar{\Sigma} + \hat{\Sigma} + \dots$  for the term in zeroth order in  $V$  and the first-order correction. There are two independent equations which look identical to Eqs. (B1) and (B2) if we replace  $1 \rightarrow 1\sigma$ ,  $2 \rightarrow 2\sigma$ , and  $12 \rightarrow 1\sigma 2\sigma$ , i.e., the equations for different spins decouple.

We calculate all diagrams explicitly and find

$$\bar{\Sigma}_{1\sigma,1\sigma}^{1\sigma,1\sigma} = \bar{\Sigma}_{2\sigma,2\sigma}^{1\sigma,1\sigma} = -i\Gamma [1 + f(\epsilon)] \quad (\text{B8})$$

$$\bar{\Sigma}_{2\sigma,1\sigma}^{1\sigma,1\sigma} - \bar{\Sigma}_{1\sigma,1\sigma}^{2\sigma,1\sigma} = \bar{\Sigma}_{1\sigma,2\sigma}^{1\sigma,1\sigma} - \bar{\Sigma}_{2\sigma,2\sigma}^{2\sigma,1\sigma} = 0 \quad (\text{B9})$$

for the terms at equilibrium, and

$$\hat{\Sigma}_{0,2\sigma}^{0,1\sigma} = \frac{\hat{\Sigma}_{1\sigma,2\sigma}^{1\sigma,1\sigma} + \hat{\Sigma}_{2\sigma,2\sigma}^{2\sigma,1\sigma}}{2} = \hat{\Sigma}_{1\sigma 2\sigma,2\sigma}^{1\sigma 2\sigma,1\sigma} = \frac{\Gamma}{2} eV f'(\epsilon) \sin \frac{\varphi}{2} \quad (\text{B10})$$

for the corrections in first order in  $V$ . This leads to

$$\hat{P}_{1\sigma}^{1\sigma} = 0 \quad (\text{B11})$$

$$\hat{P}_{2\sigma}^{1\sigma} = -\frac{i}{2} eV \frac{f'(\epsilon)}{[1 + f(\epsilon)]^3} \sin(\varphi/2). \quad (\text{B12})$$

## 3. Dot-dot interaction, no spin

Finally we consider the case of a finite interaction between dot 1 and 2. For this case, again Eqs. (B1) and (B2) hold. In the limit  $\beta\epsilon \sim 1$  but  $\beta U' \gg 1$  we find

$$\bar{\Sigma}_{1,1}^{1,1} = \bar{\Sigma}_{2,2}^{1,1} = -i\Gamma [1 - f(\epsilon)] \quad (\text{B13})$$

$$\bar{\Sigma}_{2,1}^{1,1} - \bar{\Sigma}_{1,1}^{2,1} = \bar{\Sigma}_{1,2}^{1,1} - \bar{\Sigma}_{2,2}^{2,1} = \frac{\Gamma}{\pi} \ln \frac{\beta U'}{2\pi} \cos \frac{\varphi}{2} \quad (\text{B14})$$

in equilibrium, and

$$\hat{\Sigma}_{0,2}^{0,1} = \hat{\Sigma}_{1,2}^{1,1} + \hat{\Sigma}_{2,2}^{2,1} = \frac{\Gamma}{2} eV f'(\epsilon) \sin \frac{\varphi}{2} \quad (\text{B15})$$

$$\hat{\Sigma}_{12,2}^{12,1} = 0 \quad (\text{B16})$$

for the corrections in first order in  $V$ . This leads to

$$\hat{P}_1^1 = -\frac{i}{\pi} \frac{\ln(\beta U'/2\pi)}{1 - f(\epsilon)} \cos \frac{\varphi}{2} \hat{P}_2^1 \quad (\text{B17})$$

$$\hat{P}_2^1 = -\frac{i}{2} eV \frac{f'(\epsilon)}{1 + f(\epsilon)} \cdot \frac{C}{1 - f(\epsilon)} \sin(\varphi/2) \quad (\text{B18})$$

with the factor  $C$  as defined in Eq. (4.10).

## APPENDIX C: ALTERNATIVE DERIVATION OF EQ. (4.7)

As shown in Ref. 33 the current can be written as

$$I = \frac{e}{h} \sum_{\sigma} \int d\omega \text{tr} \{ \mathbf{G}^a \mathbf{\Gamma}^R \mathbf{G}^r \mathbf{\Gamma}^L \} (f_L - f_R) \quad (\text{C1})$$

In this case for the linear conductance only equilibrium Green's functions are involved. These can be determined exactly up to all orders, e.g., by using an equations-of-motions approach. The result for the retarded Green's function is

$$G^r(\omega) = \left( \begin{array}{cc} \omega - \epsilon + i\Gamma/2 & i(\Gamma/2) \cos(\varphi/2) \\ i(\Gamma/2) \cos(\varphi/2) & \omega - \epsilon + i\Gamma/2 \end{array} \right)^{-1} \quad (\text{C2})$$

and the advanced Green's function is the complex conjugate. As a consequence the transmission is

$$T(\omega) = \frac{\Gamma^2(\omega - \epsilon)^2 \cos^2(\varphi/2)}{(\omega - \epsilon)^2 + (\Gamma/2)^2(1 + \cos(\varphi/2))^2} \times \frac{1}{(\omega - \epsilon)^2 + (\Gamma/2)^2(1 - \cos(\varphi/2))^2}. \quad (\text{C3})$$

An expansion up to first and second order in  $\Gamma$  yields

$$T^{(1)}(\omega) = \pi\Gamma\delta(\omega - \epsilon) \cos^2(\varphi/2) \quad (\text{C4})$$

for the first order, which proves Eq. (4.7), and

$$T^{(2)}(\omega) = \text{Re} \frac{\Gamma^2 \cos^2(\varphi/2)}{(\omega - \epsilon + i0^+)^2} \quad (\text{C5})$$

for the second order (cotunneling). Note that for  $\varphi = 0, \pm 2\pi, \pm 4\pi, \dots$ , the transmission in second order is twice the sum of the transmissions through the dots taken apart, as expected for constructive interference, while in first order (at resonance) no factor 2 is involved.

- 
- <sup>1</sup> H. Aker, Phys. Rev. B **47**, 6835 (1993).  
<sup>2</sup> A. Yacoby, M. Heiblum, D. Mahalu, and H. Shtrikman, Phys. Rev. Lett. **74**, 4047 (1995).  
<sup>3</sup> A.L. Yeyati and M. Büttiker, Phys. Rev. B **52**, R14360 (1995).  
<sup>4</sup> G. Hackenbroich and H.A. Weidenmüller, Phys. Rev. Lett. **76**, 110 (1996).  
<sup>5</sup> C. Bruder, R. Fazio, and H. Schoeller, Phys. Rev. Lett. **76**, 114 (1996).  
<sup>6</sup> Y. Oreg and Y. Gefen, Phys. Rev. B **55**, 13726 (1997).  
<sup>7</sup> R. Schuster, E. Buks, M. Heiblum, D. Mahalu, V. Umansky, and H. Shtrikman, Nature (London) **385**, 417 (1997).  
<sup>8</sup> W. Izumida, O. Sakai, and Y. Shimizu, J. Phys. Soc. Jpn. **66**, 717 (1997).  
<sup>9</sup> R. Baltin, Y. Gefen, G. Hackenbroich, and H.A. Weidenmüller, Eur. Phys. J. B **10**, 119 (1999).  
<sup>10</sup> R. Baltin and Y. Gefen, Phys. Rev. Lett. **83**, 5094 (1999).  
<sup>11</sup> Y. Ji, M. Heiblum, D. Sprinzak, D. Mahalu, and H. Shtrikman, Science **290**, 779 (2000).  
<sup>12</sup> W.G. van der Wiel, S. De Franceschi, T. Fujisawa, J.M. Elzerman, S. Tarucha, and L.P. Kouwenhoven, Science **289**, 2105 (2000).  
<sup>13</sup> D. Loss and E.V. Sukhorukov, Phys. Rev. Lett. **84**, 1035 (2000).  
<sup>14</sup> U. Gerland, J. v. Delft, T.A. Costi, and Y. Oreg, Phys. Rev. Lett. **84**, 3710 (2000).  
<sup>15</sup> P.G. Silvestrov and Y. Imry, Phys. Rev. Lett. **85**, 2565 (2000).  
<sup>16</sup> K. Kang and S.C. Shin, Phys. Rev. Lett. **85**, 5619 (2000).  
<sup>17</sup> D. Boese, W. Hofstetter, and H. Schoeller, Phys. Rev. B **64**, 125309 (2001).  
<sup>18</sup> A.W. Holleitner, C.R. Decker, H. Qin, K. Eberl, and R.H. Blick, Phys. Rev. Lett. **87**, 25680 (2001).  
<sup>19</sup> J. König and Y. Gefen, Phys. Rev. Lett. **86**, 3855 (2001).  
<sup>20</sup> W. Hofstetter, J. König, and H. Schoeller, Phys. Rev. Lett. **87**, 156803 (2001).  
<sup>21</sup> This is justified so long as the temperature is high enough to render the Kondo physics irrelevant.  
<sup>22</sup> D. Goldhaber-Gordon, H. Shtrikman, D. Mahalu, D. Abusch-Magder, U. Meirav, M.A. Kastner, Nature (London) **391**, 156 (1998).  
<sup>23</sup> S.M. Cronenwett, T.H. Oosterkamp, and L.P. Kouwenhoven, Science **281**, 540 (1998).  
<sup>24</sup> F. Simmel, R.H. Blick, J.P. Kotthaus, W. Wegscheider, and M. Bichler, Phys. Rev. Lett. **83**, 804 (1999).  
<sup>25</sup> J. Schmid, J. Weis, K. Eberl, and K. v. Klitzing, Phys. Rev. Lett. **84**, 5824 (2000).  
<sup>26</sup> L.I. Glazman and M.E. Raikh, Pis'ma Zh. Éksp. Teor. **47**, 378 (1998) [JETP Lett. **47**, 452 (1988)].  
<sup>27</sup> T.K. Ng and P.A. Lee, Phys. Rev. Lett. **61**, 1768 (1988).  
<sup>28</sup> Y. Meir, N.S. Wingreen, and P.A. Lee, Phys. Rev. Lett. **70**, 2601 (1993).  
<sup>29</sup> J. König, H. Schoeller, and G. Schön, Phys. Rev. Lett. **76**, 1715 (1996); J. König, J. Schmid, H. Schoeller, and G. Schön, Phys. Rev. B **54**, 16820 (1996).  
<sup>30</sup> M. Büttiker, Phys. Rev. Lett. **57**, 1761 (1986); L.J. van der Pauw, Philips Res. Rep. **13**, 1 (1958).  
<sup>31</sup> R. Landauer, Philos. Mag. **21**, 863 (1970).  
<sup>32</sup> M. Büttiker, Y. Imry, R. Landauer, and S. Pinhas, Phys. Rev. B **31**, 6207 (1985); Y. Gefen, Y. Imry, and M.Ya. Azbel, Phys. Rev. Lett. **52**, 129 (1984).  
<sup>33</sup> Y. Meir and N. Wingreen, Phys. Rev. Lett. **68**, 2512 (1992).  
<sup>34</sup> H. Schoeller, in *Mesoscopic Electron Transport*, edited by L.L. Sohn, L.P. Kouwenhoven, and G. Schön (Kluwer, Dordrecht, 1997); J. König, *Quantum Fluctuations in the Single-Electron Transistor* (Shaker, Aachen, 1999).  
<sup>35</sup> D.V. Averin and A.A. Odintsov, Phys. Lett. A **140**, 251 (1989); D.V. Averin and Yu.V. Nazarov, Phys. Rev. Lett. **65**, 2446 (1990).  
<sup>36</sup> The renormalization terms derived in second order, "cotunneling at resonance",<sup>37</sup> are negligible in this regime.  
<sup>37</sup> J. König, H. Schoeller, and G. Schön, Phys. Rev. Lett. **78**, 4482 (1997); Phys. Rev. B **58**, 7882 (1998).  
<sup>38</sup> B.L. Altshuler, A.G. Aronov, and D.E. Khmel'nitsky, J. Phys. C **15**, 7367 (1982).  
<sup>39</sup> A. Stern, Y. Aharonov, and Y. Imry, Phys. Rev. A **41**, 3436 (1990).  
<sup>40</sup> See also P.A. Mello, Y. Imry, and B. Shapiro, Phys. Rev. B **61**, 16570 (2000).  
<sup>41</sup> The regularization  $+i0^+$  is put here by hand, but can be derived within a complete cotunneling theory.<sup>37</sup>  
<sup>42</sup> Here, we have chosen  $t_L t_R \tilde{t} e^{-i\varphi}$  to be positive. If we chose a minus sign, all our conclusions would be modified in a trivial way,  $\varphi \rightarrow \varphi + \pi$ . This would modify, though, details of the evolution of the transmission phase with the gate voltage, which is not considered here.  
<sup>43</sup> This can be easily proven within a diagrammatic technique as introduced in Appendix A. The diagram of each contribution to the Green's function  $G^{(1)}$  contains one "double

vertex” describing direct tunneling through the reference arm, say from the left to the right lead. By interchanging the labels  $L$  and  $R$  for the tunnel lines connected to the double vertex we can construct another diagram which contributes to  $G^{(1)}$  as well. The double vertex now describes tunneling from right to left. Since in equilibrium the left and right leads are described by the same Fermi function, the analytic expressions for the new diagram are almost identical to the old ones. The only difference is a reversal of the AB phase,  $\varphi \rightarrow -\varphi$ , due to the exchange of the double vertex. This proves the desired symmetry relation. It is straightforward to generalize this proof for Green’s function  $G^{(n)}$  of arbitrary high order in  $t^{\text{ref}}$  and, thus, for the total Green’s function as well.

<sup>44</sup> B.L. Altshuler, Y. Gefen, A. Kamenev, and L.S. Levitov, Phys. Rev. Lett. **78**, 2803 (1997).

<sup>45</sup> T.V. Shahbazyan and M.E. Raikh, Phys. Rev. B **49**, 17123 (1994).

<sup>46</sup> J. König, Y. Gefen, and G. Schön, Phys. Rev. Lett. **81**, 4468 (1998).

<sup>47</sup> We consider here the generic case where the signs of all tunneling matrix elements  $t_{L,\text{dot}1}$ ,  $t_{L,\text{dot}2}$ ,  $t_{R,\text{dot}1}$ , and  $t_{R,\text{dot}2}$  are the same (in the absence of flux). Another choice of the relative phases among them will modify the detailed conclusions of the following analysis.

<sup>48</sup> We thank Yang Ji and M. Heiblum for discussions on this point.

<sup>49</sup> For completeness we mention that further minus signs can appear in diagrams which include states with two or more fermions. They are due to the fact that a two-vertex contribution such as  $c_{\uparrow}c_{\downarrow}^{\dagger}|\uparrow\rangle$  leads to a minus sign,  $-|\downarrow\rangle$  (see Refs. 29,34).